

On the physics of nested Markov models: a generalized probabilistic theory perspective

Xingjian Zhang¹ and Yuhao Wang^{2, *}

¹*QICI Quantum Information and Computation Initiative,*

School of Computing and Data Science, University of Hong Kong

²*Institute for Interdisciplinary Information Sciences, Tsinghua University*

Determining potential probability distributions with a given causal graph is vital for causality studies. To bypass the difficulty in characterizing latent variables in a Bayesian network, the nested Markov model provides an elegant algebraic approach by listing exactly all the equality constraints on the observed variables. However, this algebraically motivated causal model comprises distributions outside Bayesian networks, and its physical interpretation remains vague. In this work, we inspect the nested Markov model through the lens of generalized probabilistic theory, an axiomatic framework to describe general physical theories. We prove that all the equality constraints defining the nested Markov model hold valid theory-independently. Yet, we show this model generally contains distributions not implementable even within such relaxed physical theories subjected to merely the relativity principles and mild probabilistic rules. To interpret the origin of such a gap, we establish a new causal model that defines valid distributions as projected from a high-dimensional Bell-type causal structure. The new model unveils inequality constraints induced by relativity principles, or equivalently high-dimensional conditional independences, which are absent in the nested Markov model. Nevertheless, we also notice that the restrictions on states and measurements introduced by the generalized probabilistic theory framework can pose additional inequality constraints beyond the new causal model. As a by-product, we discover a new causal structure exhibiting strict gaps between the distribution sets of a Bayesian network, generalized probabilistic theories, and the nested Markov model. We anticipate our results will enlighten further explorations on the unification of algebraic and physical perspectives of causality.

I. INTRODUCTION

Understanding the relationship between various events is the everlasting theme of applied sciences. In this quest, the concept of independence is central to our reasoning. Mathematically, independence is formalized via probabilities, where the occurrence probability of an event is not affected by another. Based on this, we define correlation between variables as the opposite notion. To interpret the origin of correlations, a natural thought suggests two causal explanations: one event might have a direct causal effect on the other, and it is also possible to have unobserved issues influencing the correlated events in common. With continuous efforts to formulate these notions as rigorous mathematical expressions, we embrace the modern framework of causality in terms of algebra [1].

From a physical perspective, independence and causal effects are firmly grounded. An observer's information acquisition is reflected in the observation of events [2]. For a variable to directly influence other variables, it needs to transmit information to the latter. According to the principles of relativity theory, information transmission is subjected to the arrow of time and fundamentally restricted by the light speed in the underlying space-time [3]. Consequently, these physical notions justify the use of directed acyclic graphs (DAGs) for the study of causal influences [4, 5]. As shown in Fig. 1, a variable

is denoted as a vertex, and a direct causal influence is denoted as a directed edge.

Given a causal structure depicted by a DAG, what is the complete set of allowed correlations among observable variables? Aiming at this question, the nested Markov model provides an algebraic approach [6–8]. The nested Markov model delineates a statistical manifold with equality constraints over observable correlations. Specifically, these constraints include the usual conditional independences between random variables, which are graphically specified as the d-separation [9–11], and nonlinear constraints termed Verma's constraints [12, 13]. The nested Markov model is algebraically complete, and as proven recently, the equality constraints coincide with those in a Bayesian network with latent variables [7], where all the variables, including both the observed and unobserved ones, are entirely modelled as random variables. In other words, the nested Markov model and the Bayesian network are the same in terms of equality constraints of the observed variables, and differ only in inequality constraints [7].

Despite these appealing algebraic properties, the physical meaning of nested Markov model is largely unexplored. To our current physical understanding, observed events may originate from quantum measurements [14]. As shown by the violation of Bell inequalities, correlations beyond the reach of Bayesian networks can be generated when the latent issues admit a quantum nature [15, 16]. In exploring other plausible physical theories in accordance with relativity, generalized probabilistic theories (GPTs) have been proposed [17–19], which

* yuhaow@tsinghua.edu.cn

may support even stronger correlations between nonlocal observed variables [17, 20]. It remains vague whether the nested Markov model fully complies with the notion of independence in general physics. Moreover, by definition, the nested Markov model does not explicitly pose inequality constraints to correlations. On the other hand, as reflected by the differences in the Bell inequality violations in various physical theories, the physical modelling of causality contact restricts the strength of correlations [21]. It is unclear if the nested Markov model is too “loose,” comprising “non-physical” correlations.

In this work, we examine the physical interpretation of nested Markov models. We first prove that the equality constraints in the nested Markov model remain sound and complete for GPTs, namely, theory-independent. On the other hand, we also confirm the existence of causal structures where GPTs unavoidably pose additional inequality constraints. To better understand the gap between the nested Markov model and GPTs, we construct a new causality model standing between them. Roughly speaking, the set of correlations in the new model is defined as a specific projection result from the nested Markov model of an associated Bell-type hyper-graph. Using the new causal model, we explicitly demonstrate that the set of probability distributions encoded by GPTs contains two types of inequality constraints: one type emerges from the projection of independence conditions in the hyper graph, and the other originates from the GPT states and measurements. In other words, there are also causal structures where a strict gap exists between this projection-based and GPT causal theories. We shall provide concrete examples on this. As we will elaborate later, we suggest that the new causal model extended by the projection procedure supersedes any physically motivated causal theory.

The projection technique in constructing the new causal model allows us to borrow mature techniques in the field of Bell nonlocality to causal studies. As a by-product, by applying the projection to the multipartite nonlocal correlation in the “guess-your-neighbour’s-input (GYNI)” Bell test [22], we discover a new causal structure with a strict separation between the set of valid correlations in classical physics, GPTs and nested Markov models.

II. PRELIMINARIES

Before we commence, we first review the basic concepts of GPTs and causality. Starting from the investigation into the interpretation of quantum physics, the GPT framework was proposed to study and compare various physical theories [17]. As the name suggests, an underlying assumption of GPTs is the validity of probabilities. In statistical theory, we can abstract the essential features of probabilities and formalize the concept of a probability kernel. Following [23], given finite state spaces, $\mathcal{X}_A, \mathcal{X}_B$, a probability kernel over \mathcal{X}_A given \mathcal{X}_B is a non-negative

function

$$q : \mathcal{X}_A \times \mathcal{X}_B \rightarrow \mathbb{R}_+, \quad (1)$$

such that $\forall x_B \in \mathcal{X}_B, \sum_{x_A \in \mathcal{X}_A} q(x_A|x_B) = 1$. Moreover, we require $q(x_A|x_B) \equiv \sum_{x_C \in \mathcal{X}_C} q(x_A, x_C|x_B)$ and $q(x_A|x_B, x_C) \equiv q(x_A, x_C|x_B)/q(x_C|x_B)$. In other words, a probability kernel behaves almost like a conditional probability, except that it bypasses the marginal distribution on the indexing set \mathcal{X}_B .

Within a given physical theory under the GPT framework, an observer accesses a physical state by performing measurements on it and reading out the measurement outcomes. The measurement choice is denoted as a random variable, and the measurement outcome is described as a probability kernel over a fixed output alphabet given the measurement choice. The probability kernel must satisfy certain rules, which stem from the laws on the valid physical states and operations defining the physical theory. These laws must observe a minimal set of assumptions, as described in Box 1.

Box 1: Assumptions in GPTs [17]

Single-party system

1. The state of a single system can be determined by a probability kernel p with respect to a complete set of fiducial measurements \mathcal{F} .
2. The state set \mathcal{S} is the convex hull of the allowed normalized states and a zero state $\vec{0}$.
3. The set of allowed state transformations \mathcal{T} is formed by linear maps transforming a normalized state to a valid state.

Multipartite system

4. *Parallel composition:* If $p_A \in \mathcal{S}_A$ and $p_B \in \mathcal{S}_B$, then $p_A \otimes p_B \in \mathcal{S}_{AB}$.
5. *No-signalling:* Local operations commute.

A particular choice of \mathcal{S} and \mathcal{T} together with possibly additional assumptions specifies a GPT. Note that measurements in the set of \mathcal{F} are special physical operations belonging to \mathcal{T} . Among these assumptions, Assumptions 4 and 5, which correspond to how multiple systems compose into a joint one, shall be essential to our results. In particular, the no-signalling assumption (Assumption 5) captures the essence of relativity, where the light speed poses a fundamental limit to information transmission. If this assumption is violated, namely, local operations on different parts of a joint system are not mutually commuting, then the disturbance by an operation at one place could be instantaneously detected by a distant part of the system. This indicates information transmission faster than the light speed and violates the rules of relativity. In Appendix B, we shall further explain the assumptions in Box 1.

The GPT framework embeds the Newtonian and quantum physics. Going beyond, one of the most well-studied GPTs is the “box-world” theory [17, 20]. In brief, the box-world aims at generating the most nonlocal statistics in Bell tests subjected to relativity. In the simplest case, the Clauser-Horne-Shimony-Holt (CHSH) test [16], consider two remote non-communicating observers, Alice and Bob. The two observers share a physical state, and they each apply random measurements on their share of the state. We denote their measurement choices as random variables X and Y and their measurement outcomes as variables A and B , respectively, which all take binary values in $\{0, 1\}$. We denote the probability that the relation $X \cdot Y = A \oplus B$ is met as S . As there is no communication between the observers, each observer’s measurement result is independent of the other’s measurement choice, $X \perp\!\!\!\perp B$ and $Y \perp\!\!\!\perp A$, or written as

$$\begin{aligned} p(A = a|X = x) &= \sum_b p(A = a, B = b|X = x, Y = y) \\ &= \sum_b p(A = a, B = b|X = x, Y = y'), \\ p(B = b|Y = y) &= \sum_a p(A = a, B = b|X = x, Y = y) \\ &= \sum_a p(A = a, B = b|X = x', Y = y). \end{aligned} \quad (2)$$

In the following, we abbreviate $p(A = a|X = x)$ as $p(a|x)$ and take a similar convention when there is no ambiguity. When the physical processes are subjected to classical physics, there is an upper bound of $S \leq 3/4$ [16]. Quantum theory allows a higher value of it, exhibiting nonlocal correlations among the variables. However, S is upper-bounded by $S \leq (2 + \sqrt{2})/4$, still strictly away from unity [24]. The box-world theory closes this gap. Assume all the probability distributions $p(a, b|x, y)$ satisfying the constraints in Eq. (2) represent valid physical processes on a bipartite state. Then, the following probability distribution represents a no-signalling physical process yielding a perfect correlation of $S = 1$:

$$p(a, b|x, y) = \frac{1}{2} \delta_{a \oplus b = xy}. \quad (3)$$

In the literature, this probability distribution is usually cited as the Popescu-Rohrlich (PR) box [20].

As mentioned above, DAGs provide a useful tool to visualize the causal structure among various variables in an event [5]. The parental vertex in an edge represents the cause, and the child vertex represents the effect. In Fig. 1(a), we depict the DAG for the CHSH Bell test. In classical causality, all the vertices, including observable and latent variables, are characterized as random variables, and causal influences are fully characterized by conditional probabilities. In this case, the causal model is also called a Bayesian network. In a quantum or more general GPT causal theories, the latent variables correspond to the physical states in the underlying physical

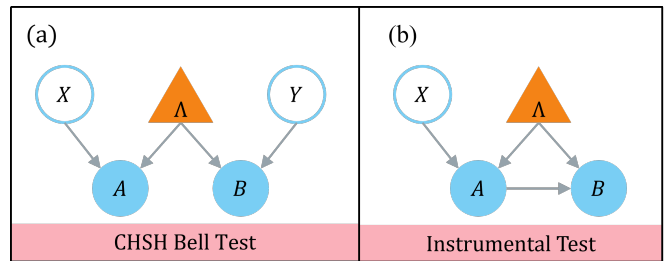


FIG. 1. DAGs for the CHSH Bell test and the instrumental test. In the DAG of a causal structure, nodes represent variables, and directed edges represent causal influences, where the parental node represents the cause and the child node represents the effect. We distinguish observable variables from latent ones, as denoted by blue circles and orange triangles, respectively. (a) The CHSH Bell test causal structure. The nodes X and Y represent the measurement choices of the observers, A and B represent the measurement outcomes, and Λ represents the latent variable, which is common cause of A and B . In the CHSH test, all the observable variables take binary values. (b) The instrumental test causal structure. The node X represents the instrumental variable, A and B are considered to be the direct cause and effect, and Λ is the latent variable, which is common cause of A and B .

theory [25]. Correspondingly, an observable variable with an incoming edge from the latent variable should be interpreted as the outcome of a measurement. Besides, a parental observable variable can serve as a classical control for the measurements. In Appendix C, we shall rigorously state the physical interpretation of causal DAGs in GPTs. Given a causal structure G , when the underlying physical theory is the Newtonian physics, we denote the set of valid probability distributions among observed variables as $\mathcal{C}(G)$. We remark that in this work, we only consider causal structures where latent variables correspond to the root vertices. Analogously, given any physical theory within the GPT framework, we can obtain a set of valid probability distributions, whose union is denoted as $\mathcal{GPT}(G)$. As a special GPT, for the box-world theory, we denote the set of probability distributions as $\mathcal{NS}(G)$. As shown in the CHSH Bell test, we have the strict inclusion $\mathcal{C}(G) \subsetneq \mathcal{NS}(G)$ in general.

To characterize plausible correlations in a causal structure, we are first interested in the independence conditions among observed random variables. In a Bayesian network, all the conditional independences can be enumerated from the Bayesian rules of probability calculation. For instance, in Fig. 2(a), as the causal influence of X on B is mediated by A , we have the conditional independence of $X \perp\!\!\!\perp B|A$, or the Markov condition:

$$p(x, a, b) = p(x)p(a|x)p(b|a). \quad (4)$$

Alternatively, DAGs provide a graphical criterion to specify these conditional independences, equivalently stated as the d-separation [5]. In brief, denote a pseudo path between two vertices as a sequence of edges linking them without two consecutive ones directing towards

the same intermediate vertex. Here, the edges and vertices may involve the latent variables. Two vertices are d-separated from each other if they are not linked by a pseudo path, or d-separated by a set of vertices if the latter block all their linking pseudo paths. While originally developed for the study of Bayesian networks, the d-separation holds for generalized latent variables to tell the statistical conditional independence conditions between observable variables [25]. For a causal structure characterized by a DAG G , we denote the set of probability distributions of observable variables whose conditional independence statements are consistent with the d-separation statements in G as $\mathcal{I}(G)$. In Henson *et al.* [25], it has been proved that $\mathcal{GPT}(G) \subseteq \mathcal{I}(G)$. In other words, the conditional independence conditions among observed variables are theory-independent.

III. NESTED MARKOV MODEL IN GENERALIZED PROBABILISTIC THEORIES

As an equality constraint, each conditional independence condition in a causal structure, or equivalently, a d-separation condition, reduces a dimension of the statistical manifold for the set of valid distributions. However, in the study of Bayesian networks, it is found that there are other equality constraints in general. Consider the causal structure of the mediation test in Fig. 2(a) and assume Λ is a classical random variable for now. Using the Bayesian formula, one can prove the following expression

$$q(c|b) \equiv \sum_{A=a} p(a|x)p(c|x, a, b) \quad (5)$$

is a function of only B and C , independent of X . Such an equality is called the Verma constraint [12, 13]. Different from the usual conditional independence conditions between random variables, the Verma constraint cannot be identified through the d-separation statements in G .

In classical causal theory, given a causal structure G , the set of probability distributions that satisfy all the usual conditional independence conditions and Verma constraints is considered as the nested Markov model associated with G [7, 8], which we denote as $\mathcal{N}(G)$. The nested Markov model is proven to provide an algebraically complete description of the Bayesian network with latent variables, listing exactly all the equality constraints among observed variables [7]. Namely, $\mathcal{C}(G)$ and $\mathcal{N}(G)$ define manifolds in the probability simplex that are equivalent up to the difference of inequality constraints. Since a classical causal structure usually poses additional constraints, we have $\mathcal{C}(G) \subseteq \mathcal{N}(G)$, and there are causal structures making the inclusion strict.

The original derivation of Verma constraints is restricted to Bayesian networks [12, 13]. In this proof, besides the observed variables, the latent variables are also characterized as classical random variables. Verma

constraints are obtained by decomposing the overall distribution of all the variables with respect to the usual Markov condition, applying the Bayes rule, and finally marginalizing over the distribution of latent variables. It is less clear whether Verma constraints and hence the nested Markov model remain valid for GPT causal theories. As suggested by the proven validity of d-separation in GPTs [25], it is tempting to consider the Verma constraints as properties inherent to a causal structure, independent of the underlying physical theory. Here, we confirm this statement positively.

Theorem 1 (Nested Markov property in GPTs). *Consider a causal structure defined by DAG G , where the latent variables represent physical states in some GPT. Any possible probability distribution over the observable vertices satisfies all the Verma constraints for G . Consequently, $\mathcal{GPT}(G) \subseteq \mathcal{N}(G)$.*

In previous studies, a graph-based recursive procedure was proposed to find all the Verma constraints [6, 7]. Previous research has proven this procedure's validity under classical physical theory, where the observed distribution can be described by a Bayesian network. We prove this graph-based procedure remains valid theory-independently, leading to Theorem 1.

As an example, we show how the procedure works for the mediation test in GPTs, whose causal structure is depicted in Fig. 2(a). Suppose there is a probability distribution $p(x, a, b, c)$ among observed variables. When the DAG represents a classical Bayesian network, then $p(x, a, b, c)$ represents a marginal distribution of $p(x, a, b, c, \lambda)$, where λ corresponds to the latent random variable Λ . Graphically, we may depict the marginal distribution $p(x, a, b, c)$ as a marginal DAG (mDAG) in Fig 2(b), where the latent variable Λ being marginalized over is replaced with a bi-directed edge [7, 26]. Applying the Bayes rule to the joint probability of all the variables and finally marginalizing the latent variable, $p(x, a, b, c)$ can be factorized as:

$$p(x, a, b, c) = p(x)p(b|a)q(a, c|x, b), \quad (6)$$

where $q(a, c|x, b)$ represents a valid probability kernel over \mathcal{X}_A and \mathcal{X}_C given \mathcal{X}_X and \mathcal{X}_B . Moreover, this kernel satisfies

$$q(c|b) = \sum_a q(a, c|x, b). \quad (7)$$

In other words, $q(a, c|x, b)$ can be described by the sub-graph shown in Fig 2(c): the vertex A is a collider in the path linking X and (B, C) ; thus marginalizing A results in independence between X and (B, C) . In Appendix D, we prove that beyond Bayesian networks, when Λ represents a generalized physical state in a GPT, we still have a factorization as (6), and $q(a, c|x, b)$ remains a valid probability kernel and satisfies the marginalization in (7), merely with a different physical origin relying on the underlying GPT. In other words, the graphical representation of the procedure remains the same. Applying the

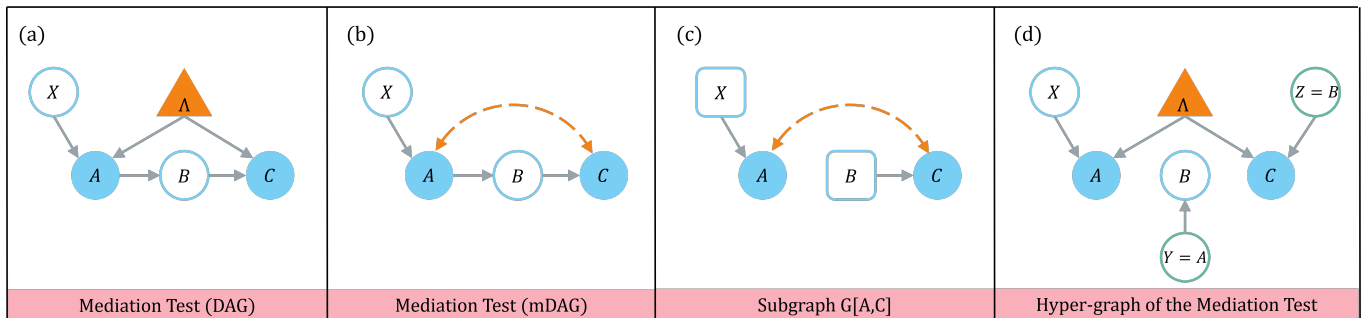


FIG. 2. Analysis for the mediation test causal structure. (a) DAG of the mediation test. The causal structure includes observable variables X, A, B , and C , and a latent variable Λ . This is the simplest structure exhibiting the Verma constraint. (b) The mDAG for the mediation test. The latent variable Λ that is the common latent cause of A and B is abstracted into a simplicial complex denoted by a bi-directed arrow. The mDAGs were used in Evans [7] to represent the nested Markov models. (c) A subgraph of the mDAG, which graphically depicts the probability kernel $q(a, c|x, b)$, a term in the decomposition of Eq. (6). (d) The hyper-graph with a low-dimensional projection to the mediation test. The green hollow circles are added nodes in the hyper-graph, and a data post-selection of $Y = A$ and $Z = B$ projects the structure back to the mediation test.

Bayes rule to the observed probability $p(x, a, b, c)$, one can easily check that

$$q(a, c|x, b) = p(a|x)p(c|a, b), \quad (8)$$

which is the expression to be summed over in Eq. (5). Note that we do not need to characterize the latent variable Λ to obtain (8). Therefore, we arrive at the Verma constraint in Eq. (5). In Appendix D, we provide the formal statement of the graph-based procedure for general causal structures and rigorously prove Theorem 1.

IV. A CAUSAL MODEL BETWEEN THE NESTED MARKOV MODEL AND GPTS

While the nested Markov model fully covers the predictions of GPTs, we shall show that the converse is not true. Namely, there exist causal structures such that $\mathcal{GPT}(G) \subsetneq \mathcal{N}(G)$. This is expected as the nested Markov model is defined solely by equality constraints in the probability space. On the other hand, the requirement of “physical” states and operations in a GPT poses non-trivial inequality constraints. In other words, GPTs do not provide the exact physical interpretation of the nested Markov model.

Before discussing concrete examples of causal structures, we construct a new causal model whose probability space stems solely from conditional independence. Notably, the new model stands in between $\mathcal{GPT}(G)$ and $\mathcal{N}(G)$. Besides, the new model has its own interests in unveiling the algebraic origins of certain causality constraints. To introduce the new causal model, we first define operations of a causality DAG extension and projection.

Definition 1. Consider a causal structure denoted by a DAG $G(V, W, \mathcal{E})$, where V is the set of vertices representing observed variables, W is the set of vertices representing latent variables, and \mathcal{E} is the edge set. Label all the

vertices in V with an index set $[n] = \{1, \dots, n\}$. From $i = 1$ to $i = n$, perform the following operations if $v_i \in V$ has both incoming edges from $V \cup W$ and outgoing edges to other vertices in V :

1. remove all its outgoing edges $v_i \rightarrow \text{ch}(v_i) \subseteq \mathcal{E}$, where $\text{ch}(v_i) = \{v_{i,j}\}_{j=1}^{J_i} \subseteq V$ is the set of child vertices of v_i in V ;
2. for each child vertex $v_{i,j}$ of v_i , add a root vertex $u_{i,j}$ and equip it with a classical variable $X_{i,j}$ sharing the same marginal distribution as X_i and a directed edge $u_{i,j} \rightarrow v_{i,j}$;

We denote the set of vertices $u_{i,j}$ as U ; and denote the set of remaining edges as well as new edges as \mathcal{E}' . The result of the above procedure is defined as the hyper DAG $H(G)(V \cup U, W, \mathcal{E}')$ associated to G .

Remark 1. We would like to note that the hyper-graph construction introduced in Def. 1 is quite similar to the Single World Intervention Graph (SWIG) construction discussed by Richardson and Robins [27]. However, since the concept of potential outcomes is not widely known in the physics community; moreover, the physical meaning of potential outcomes seems not very well clear in non-classical physical systems, such as quantum systems; we have decided not to adopt this approach in Def. 1.

We give an example in Fig. 2(d), where $A \rightarrow B$ is replaced with $Y \rightarrow B$, and $B \rightarrow C$ is replaced with $Z \rightarrow C$, with Y, Z being the newly added vertices. With the additional vertices introduced in the definition of $H(G)$, every vertex is now either a root or an end one. This makes $H(G)$ a Bell-type DAG, though there might be more than one latent variables. Now consider the set of valid correlations among observed vertices in the vertex sets V and U of the hypergraph $H(G)$. Within a particular GPT \mathcal{G} , we can define the latent state space of $H(G)$ in a straightforward way, where each latent vertex in W is equipped with the set of all valid physical

states. Accordingly, every vertex in V and U simply represents either a measurement choice or a measurement result (note that trivial measurements might exist, such as the case of Y and B in Fig. 2(d)). We define the set of valid correlations among observed vertices in $H(G)$ within GPT \mathcal{G} as $\mathcal{G}(H(G))$. We first inspect the equality constraints of $H(G)$ for algebraic soundness, which should be respected by every GPT. Our first observation is that the equality constraints of $H(G)$ are the same as its conditional independence constraints.

Proposition 1. *For any DAG G , there is no Verma constraint in the causal structure defined by its hypergraph $H(G)$. Consequently, $\mathcal{N}(H(G)) = \mathcal{I}(H(G))$.*

We leave the proof of this proposition in Appendix E1. Note that when G is already a Bell-type graph, we trivially have $H(G) = G$. Once we further have that G has only one latent variable, $\mathcal{I}(G) = \mathcal{NS}(G)$, which is the set of correlations obtainable by the box-world GPT.

As can be expected, the correlation set of hypergraph $H(G)$ should be closely related with that of the original graph G . To formalize the statements, we first define a distribution projection operation.

Definition 2. *Given a causality DAG G and its associated hypergraph $H(G)$ obtained from Def. 1, within a particular GPT \mathcal{G} , consider a valid probability kernel among observed variables $p(X_V, X_U)$, where $X_V = \{X_1, \dots, X_n\}$, and $X_U = \{X_{\ell_1,1}, \dots, X_{\ell_1, J_{\ell_1}}, \dots, X_{\ell_m,1}, \dots, X_{\ell_m, J_{\ell_m}}\}$, where $\{\ell_1, \dots, \ell_m\}$ is the index of the set of observed vertices in G having both incoming and outgoing edges. Given p , a distribution of $p(X_V, X_U)$, we write the projected probability $P(p)$ as the distribution of X_V conditional on the event $\cap_{i=1}^m \{X_{\ell_i} = X_{\ell_i,1} = \dots = X_{\ell_i, J_{\ell_i}}\}$:*

$$P(p) = p\left(X_V \mid \cap_{i=1}^m \{X_{\ell_i} = X_{\ell_i,1} = \dots = X_{\ell_i, J_{\ell_i}}\}\right). \quad (9)$$

It can be easily checked that $P(p)$ is also a probability kernel. With a slight abuse of the notation, we denote $P(\mathcal{G}(H(G)))$ as the set of probability kernels projected from $\mathcal{G}(H(G))$, which is the set of valid correlations in $H(G)$ subjected to GPT \mathcal{G} . This projection has the following property.

Proposition 2. *For every GPT \mathcal{G} respecting assumptions in Box 1 and every causal structure G , we have*

$$\mathcal{G}(G) = P(\mathcal{G}(H(G))). \quad (10)$$

Consequently,

$$\mathcal{GPT}(G) = \bigcup_i \mathcal{G}_i(G) = P(\mathcal{GPT}(H(G))). \quad (11)$$

The proof is quite intuitive. Since we only add vertices corresponding to observed variables, the effect on any original vertex in G is not changed. Specifically, the outgoing systems of each latent variable remain the same; for each observed vertex v in G , its incoming systems remain the same; and for every measurement choice, the physical measurement performed on the system is the same. We leave the formal proof in Appendix E2.

Now, let us inspect the operations in Def. 1 and 2. Physically, $\mathcal{I}(H(G))$ is defined via conditional independence constraints, thereby representing the minimal requirement to define the physical rules of calculating a probability kernel in consistency with relativity principles. Furthermore, as shown by Proposition 1, $\mathcal{I}(H(G))$ provides a complete algebraic characterization of the equalities in $\mathcal{GPT}(H(G))$. Based on these facts and in light of Proposition 2, we are encouraged to define the following causal model.

Definition 3. *Consider a causality DAG G . Define the causal model $\mathcal{PS}(G)$ as the set of probability kernels:*

$$\mathcal{PS}(G) = P(\mathcal{I}(H(G))). \quad (12)$$

In Def. 3, the “ \mathcal{PS} ” stands for “post-selection”, since the conditioning in Def. 2 essentially constitutes a form of selection. Using Propositions 1 and 2 and Theorem 1, we can derive the following relationship between GPTs, the nested Markov model, and the new causal model.

Lemma 1. *For any DAG G , $\mathcal{GPT}(G) \subseteq \mathcal{PS}(G) \subseteq \mathcal{N}(G)$.*

In Appendix E3, we provide the complete proof of Lemma 1. While the equality constraints in these causal models are the same, it remains to check whether there are non-trivial inequality constraints that separate them. For the simple causal structures with one latent variable, where $H(G)$ represents a standard Bell test and $\mathcal{I}(H(G)) = \mathcal{NS}(H(G))$, we have the following result.

Lemma 2. *If G is a graph that has only one latent variable, then $\mathcal{GPT}(G) \equiv \mathcal{PS}(G) = \mathcal{NS}(G)$. Moreover, there exist such causal structures where $\mathcal{PS}(G) \subsetneq \mathcal{N}(G)$.*

We prove the equality part in Appendix E4. To exhibit the separation, consider the renowned instrumental scenario [28] shown in Fig. 1(c). Suppose all the observable variables take binary values in $\{0, 1\}$. We can relate the instrumental scenario with the CHSH Bell test in Fig. 1(a). By projecting the Bell test to the original causal structure, one can find that the following inequality holds for $\mathcal{PS}(G)$ and hence for any GPT [25, 29]:

$$\max_a \sum_b \max_x p(a, b|x) \leq 1. \quad (13)$$

However, the instrumental test is so simple that except for the normalization of probability kernels, no equality

constraint among the observable variables exists; thus the nested Markov model $\mathcal{N}(G)$ and $\mathcal{I}(G)$ for this structure are trivially described by the entire probability space. In this case, we have the strict inclusion of $\mathcal{GPT}(G) = \mathcal{PS}(G) \subsetneq \mathcal{N}(G) = \mathcal{I}(G)$.

The above example suggests that the nested Markov model is sometimes “too loose” to accurately describe the correlations in a causal structure. On the other hand, there exist causal structures where GPTs seem “too strict,” which also leads to $\mathcal{GPT}(G) \subsetneq \mathcal{N}(G)$. For this purpose, we look into causal structures with more than one latent variables. Consider the causal structure in Fig. 3(a), which corresponds to the entanglement swapping scenario in quantum information [30]. In this structure, $\mathcal{PS}(G) = \mathcal{N}(G) = \mathcal{I}(G)$, which are determined by the independence conditions $X \perp\!\!\!\perp \{B, C, Z\}$, $Z \perp\!\!\!\perp \{X, A, B\}$, $A \perp\!\!\!\perp C$. The following probability distribution

$$p(A = a, C = c | B = 0, X = x, Z = z) = \frac{1}{2} \delta_{a \oplus c = xz} \quad (14)$$

is an allowed correlation in $\mathcal{PS}(G)$. However, this distribution lies outside $\mathcal{GPT}(G)$, where there is no GPT generating such statistics from its valid physical states Λ_1, Λ_2 and proper operations. We prove this result by slightly generalizing the analysis within the box-world theory [31] in the proof of Theorem 2 in Appendix E5.

To summarize, in Table I, we compare the constraints in the causal models $\mathcal{N}(G)$, $\mathcal{PS}(G)$, and $\mathcal{GPT}(G)$. Indeed, these models all share the same equality constraints, encompassing all the equality constraints of a Bayesian network. Nevertheless, they differ in inequality constraints. In the first level, the nested Markov model $\mathcal{N}(G)$ does not specify any inequality constraint and is thus the loosest set among the three models. In the second level, $\mathcal{PS}(G)$ characterizes the constraints in G by extending it to a high-dimensional hypergraph, inspecting the conditional independences therein, and projecting the constraints back to the original structure. As shown in the instrumental scenario, besides generating all the equality constraints, what is remarkable is that inequality constraints in the low-dimensional structure can emerge from the projection of conditional independences in a high-dimensional structure, which are equality constraints. In this sense, $\mathcal{PS}(G)$ suggests that the nested Markov model $\mathcal{N}(G)$ contains some “unphysical” probability kernels, as it overlooks some indications of independences, and thus violates the relativity principle. Finally, in $\mathcal{GPT}(G)$, “physical requirements” on states and operations can pose stringently additional inequality constraints not in $\mathcal{PS}(G)$. At this stage, the physical meanings of the distributions in $\mathcal{PS}(G) \setminus \mathcal{GPT}(G)$ is less clear; nevertheless, we hope the construction of $\mathcal{PS}(G)$ can help us reflect the notion of causality and better understand the origin of the gap between algebraically and physically motivated causal models.

Notwithstanding, we also remark that $\mathcal{PS}(G)$ may be further tightened. Consider the triangle scenario shown

Constraints	Model		
	$\mathcal{N}(G)$	$\mathcal{PS}(G)$	$\mathcal{GPT}(G)$
equalities	✓	✓	✓
relativity-induced inequalities	×	✓	✓
theory-induced inequalities	×	×	✓

TABLE I. Comparison between $\mathcal{N}(G)$, $\mathcal{PS}(G)$, and $\mathcal{GPT}(G)$. Here “relativity-induced inequalities” means that these inequalities originates from the projection of the conditional independence constraints in the hyper-graph, which is introduced in accordance with the relativity principal. “theory-induced inequalities” means that these inequalities are given by the additional definitions of state space and measurement operations driven by GPT theory.

in Fig. 3(b). There is not any independence constraint among the observable random variables, A, B , and C ; hence $\mathcal{N}(G)$ is equal to the entire probability space. In addition, the causal structure cannot be lifted to a non-trivial hyper-graph in Def. 3, indicating that $\mathcal{PS}(G)$ is also trivially defined. Yet, as the observable events are linked with each other non-trivially, a physical intuition suggests limitations on the correlation strength. Indeed, using the entropic inequality [25], the fully symmetric probability distribution

$$p(a, b, c) = \begin{cases} \frac{1}{2}, & \text{if } a = b = c = 0, \\ \frac{1}{2}, & \text{if } a = b = c = 1, \\ 0, & \text{otherwise} \end{cases} \quad (15)$$

is found invalid in any GPT causal theory. In this case, we have the strict inclusion of $\mathcal{GPT}(G) \subsetneq \mathcal{PS}(G) = \mathcal{N}(G)$. It was recently noticed that by constructing hyper-graphs that add not only observable vertices but also latent ones, a general procedure called inflation [32, 33], inequality constraints can arise [34]. Nevertheless, such constructions require a more rigorous thinking of independence between latent variables and the parallel composition assumption in Box 1. We leave the more fine-tuned causal models for future study.

To summarize our findings, we present the following theorem.

Theorem 2. *For any causal structure denoted as DAG G , the following inclusions always hold:*

$$\mathcal{C}(G) \subseteq \mathcal{GPT}(G) \subseteq \mathcal{PS}(G) \subseteq \mathcal{N}(G) \subseteq \mathcal{I}(G). \quad (16)$$

Moreover, there exists a causal structure that makes all the inclusions strict.

V. A MINIMAL CAUSAL STRUCTURE SEPARATING CAUSAL MODELS

As is extensively explored in Bell nonlocality, we are interested in finding causal structures where different physical theories pose different constraints to the correlations

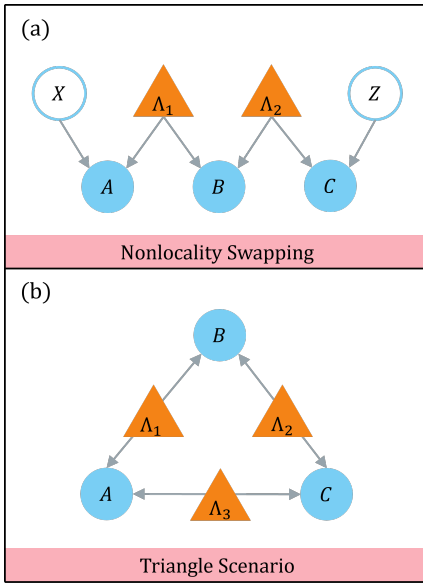


FIG. 3. Two causal structures where $\mathcal{GPT}(G) \subsetneq \mathcal{PS}(G)$. (a) The nonlocality swapping causal structure. The circles represent observable variables, including X, A, B, C , and Z , and the triangles represent the latent variables, including Λ_1 and Λ_2 . (b) The triangle causal structure. The circles represent observable variables, including A, B , and C , and the triangles represent the latent variables, including Λ_1, Λ_2 , and Λ_3 .

among observed variables. In this section, we find a new DAG such that

$$\mathcal{C}(G) \subsetneq \mathcal{GPT}(G) \subsetneq \mathcal{N}(G). \quad (17)$$

For this purpose, we take advantage of the new causal model, $\mathcal{PS}(G)$. Notably, this causal structure contains four observable nodes and one latent node, and the above inclusions already hold when all the observable variables take binary values. To our best knowledge, with the same number or fewer nodes and observable variables taking binary values, the only other causal structure that has been proven to exhibit $\mathcal{C}(G) \subsetneq \mathcal{GPT}(G)$ is the CHSH Bell test in Fig. 1(a), yet it does not exhibit a strict separation between $\mathcal{GPT}(G)$ and $\mathcal{N}(G)$. In a sense, the new structure is a minimal one separating $\mathcal{C}(G), \mathcal{GPT}(G)$, and $\mathcal{N}(G)$. Nevertheless, we remark that when the observed variables take larger alphabets, $\mathcal{C}(G) \subsetneq \mathcal{GPT}(G)$ is known for the instrumental scenario [35], the triangle scenario [36], and a causal structure known as Evans' scenario [26, 37], all containing three observed variables.

Consider the DAG G shown in Fig. 4(b), with $X, A, B, C \in \{0, 1\}$. In this causal structure, a latent variable Λ simultaneously affects observables A, B , and C . An exogenous variable X directly affects A , which is mediated by B to be carried to C . From Proposition 1, we have $\mathcal{GPT}(G) = \mathcal{PS}(G)$. It can be checked that the structure does not have any non-trivial equality constraints among observed variables. Hence, $\mathcal{N}(G) = \mathcal{I}(G)$, spanning the entire probability simplex. As G contains the instrumental scenario as a sub-structure, where the

no-signalling condition poses the non-trivial condition in Eq. (13) on the observational data, $\mathcal{GPT}(G)$ is a strict subset of $\mathcal{N}(G)$.

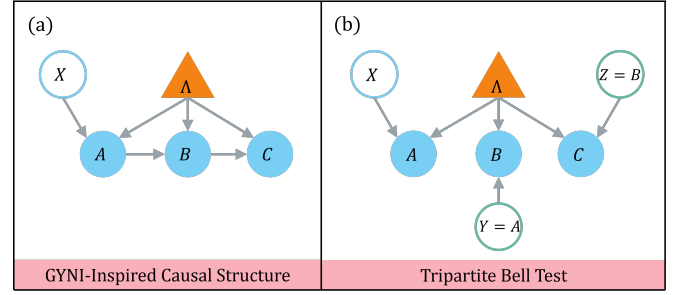


FIG. 4. (a) A causal structure with $\mathcal{C}(G) \subsetneq \mathcal{GPT}(G) \subsetneq \mathcal{N}(G)$. The circles represent observable variables, including X, A, B , and C , and the triangle represents the latent variable Λ . (b) The high-dimensional hyper-graph of (a). The green hollow circles are added nodes in the hyper-graph, and a data post-selection of $Y = A$ and $Z = B$ projects the structure back to the original scenario.

To show the strict inclusion of $\mathcal{C}(G) \subsetneq \mathcal{GPT}(G)$, we look into the corresponding hyper-graph of G . As shown in Fig. 4(a), the high-dimensional structure represents the tripartite standard Bell test with input variables X, Y , and Z , which set random measurements on a tripartite physical state Λ with measurement results A, B , and C , respectively. In the tripartite Bell test, there exist no-signalling nonlocal statistics, which represent valid physical states in the box-world GPT, that cannot be generated by any classical or even quantum operations [22]. One such distribution is given by

$$p(a, b, c | x, y, z) = P_1(a, b, c | x, y, z) \equiv \frac{1}{3} f(a, b, c, x, y, z),$$

$$f(a, b, c, x, y, z) = (1 \oplus b \oplus x \oplus y \oplus xy)(1 \oplus c \oplus z) \oplus a(1 \oplus y \oplus cy \oplus b(c \oplus z)), \quad (18)$$

where $X, Y, Z, A, B, C \in \{0, 1\}$. Intuitively, these statistics can be understood as an optimal strategy to play a nonlocal game called “guess your neighbour’s input” (GYNI) [22], where three nonlocal players win the game if and only if $A = Y, B = Z$, and $C = X$, namely, each player’s output makes a correct guess of their neighbour’s input. Except $C = X$, the winning condition is inherently similar to the projection technique in the causality study. Consequently, we obtain a set of valid statistics in $\mathcal{NS}(G)$:

$$p(a, b, c | x) = P_1(a, b, c | x, y = a, z = b), \quad (19)$$

with

$$p(a, b, c | x) = \begin{cases} \frac{1}{3}, & \text{if } (a, b, c) = (0, 0, 0), (1, 0, 1), (1, 1, 0) \text{ when } x = 0, \\ \frac{1}{3}, & \text{if } (a, b, c) = (0, 1, 1), (1, 0, 1), (1, 1, 0) \text{ when } x = 1, \\ 0, & \text{otherwise.} \end{cases} \quad (20)$$

By running a linear programming, we find this set of statistics lies outside $\mathcal{C}(G)$, thus proving $\mathcal{C}(G) \subsetneq \mathcal{GPT}(G)$. In Appendix F, we present the detailed analysis for this result.

VI. DISCUSSIONS AND OUTLOOK

In this work, we study the physical interpretation of the nested Markov model, an algebraic approach to causality characterization. For this purpose, we look into GPTs, where latent variables may represent generalized physical states subjected to certain probabilistic rules and relativity principles. Given a causal structure, the nested Markov model is specified by equality constraints among observable variables, including the (conditional) independence conditions and Verma constraints. With the help of a graph-based definition of nested Markov models, we prove all these equality constraints are sound and complete regardless of the underlying physics. Consequently, GPT causal theories comply with the nested Markov model. On the contrary, we show causal structures in which the nested Markov model allows “non-physical” probability distributions among observable variables.

To understand the gap between the nested Markov model and GPTs, we construct a new causal model, where every causal structure is considered a low-dimensional projection from a high-dimensional Bell-type structure. All the equality constraints originate from the projection of usual conditional independence conditions among relevant observable variables in the high-dimensional structure. The new model also predicts the emergence of inequality constraints from the projection of conditional independence conditions, strengthening the nested Markov model by further restricting the volume of statistical manifolds. However, GPTs still seem “too strict” compared to the new causal model; since as shown in the nonlocality swapping problem, causal structures with more than one latent variable, GPTs may pose additional inequality constraints due to the requirement of “physical operations”. While we suggest the new model supersedes any physically well-motivated causal theory, we anticipate an intermediate causal theory between the GPTs and the current model, which fully respects the causal structures and closes the gap between the algebraic and physical perspectives. One possibility is to consider hyper-graphs, adding not only observable variables but also latent ones. Some progress has been made in this direction [33, 34]. In a more radical attempt, as has been explored in some gravity theories, the underlying assumption of probabilities may be relaxed or even dropped [38, 39].

Finally, inspired by GYNI and the projection technique, we discover a minimal causal structure separating Bayesian networks, GPTs, and the nested Markov model. While the new structure is a common substructure of larger ones, it is appealing to develop systematic

criteria to determine whether a general causal structure manifests a gap between the predictions in various causal theories [25]. In addition, we restrict our discussion to binary observable variables. We look forward to further study of the effect of variable alphabets on causal theories.

VII. ACKNOWLEDGEMENT

We acknowledge Lorenzo Giannelli, Yuwei Zhu, and Yuan Liu for the insightful discussions. XZ acknowledges support by the Hong Kong Research Grant Council (RGC) through grant number R7035-21, SRFS2021-7S02, No. 27300823, and N_HKU718/23, HKU Seed Fund for Basic Research for New Staff via Project 2201100596, Guangdong Natural Science Fund via Project 2023A1515012185, National Natural Science Foundation of China (NSFC) via Project No. 12305030 and No. 12347104, and Guangdong Provincial Quantum Science Strategic Initiative GDZX2200001.

Appendix A: Table of Contents

In the Appendix, we provide the details that lead to the results in the main text. In Appendix B, we review the formulation of generalized probabilistic theories (GPTs) and discuss the physical motivation of this framework. In Appendix C, we review the causality description in GPTs, which shall provide the basic toolkit for our derivations. In Appendix D, we prove the first main result in this work, Theorem 1, showing that the nested Markov model supersedes GPTs. In Appendix E, we analyse our new causal model based on a projection technique, proving the results of Propositions 1 and 2, Lemmas 1 and 2. Finally, in Appendix F, we analyse the new causal structure inspired by the projection-based causal model and the “guess-your-neighbour’s-input” nonlocal game, proving its non-classical property.

Appendix B: GPT Formulation

We first make a few remarks on the GPT framework used in this work. First, the assumptions of convexity and no-signalling condition are important for causality discussions [18]. A vital fact is that these assumptions lead to the notion of a unique “deterministic effect”, which prevents an event to affect previous ones that are well-defined in the spacetime. We shall show the exact definition of the deterministic effect later. A simple example is the ignorance of an event, which corresponds to a variable with a definite value that trivially indicates the existence of “something”.

Second, the GPTs subjected to assumptions in Box 1 are considered “complete GPTs”; namely, such a GPT first specifies the set of allowed states \mathcal{S} , including the single-party systems and multipartite systems. The set of allowed transformations includes all the well-defined linear transformations, which maps a valid state that may be a part of a multipartite system to a valid state. This assumption is sometimes called the “no-restriction rule” [40], as the set of valid physical operations is mathematically the largest. In some results, the set of valid physical operations is further restricted by some physically motivated requirements [40–42]. In addition, a large variety of GPTs are also required to satisfy the local tomography requirement, where the global state of a multipartite system can be completely determined by specifying joint probabilities of outcomes for fiducial measurements performed simultaneously on each subsystem [17]. A well-known GPT that fails to satisfy local tomography is the real-valued quantum theory [43]. Nevertheless, the no-restriction rule and the removal of local tomography only pose restrictions to the set of valid correlations within a causal structure. As we aim to minimize the gap between GPTs and algebraically motivated causal models, it suffices to consider complete GPTs.

To see how the GPT framework works, we take the standard quantum theory as an example [14]. A valid

state in quantum theory is characterized as a density operator, which is a semi-definite positive operator with a unit trace. The state set comprises all the density operators, which is a convex set. Valid state transformations are characterized by completely positive and trace-preserving maps, or quantum channels, which also form a convex set. Quantum measurements, which are special quantum channels, can be generally described as positive operator-valued measures (POVMs). When measuring a quantum state ρ with a POVM $\{M_i\}_i$, where the POVM elements satisfy $M_i \geq 0$, $\sum_i M_i = I$, the measurement outcome i is obtained with probability $p_i = \text{tr}(\rho M_i)$. The zero state can be described by an event that does not occur in the measurement. For a single-party state, by applying an information-complete state tomography, such as the measurements formed by the eigenvectors of Pauli operators $\sigma_x, \sigma_y, \sigma_z$ in the qubit case, the state can be fully characterized via the measurement outcome probabilities. The fiducial measurements thus correspond to the quantum measurements for tomography. When physical operations act on different subsystems of a state ρ , if no communication is made during the process, the resulted state is irrelevant of the order taken by the operations. Consider measurements $\{M_i\}_i$ and $\{N_j\}_j$ on separate parts of a bipartite state ρ . The probability of outcome (i, j) is given by

$$\begin{aligned} p(i, j) &= \text{tr}[\rho(M_i \otimes I)(I \otimes N_j)] \\ &= \text{tr}[\rho(I \otimes N_j)(M_i \otimes I)] \\ &= \text{tr}[\rho(M_i \otimes N_j)]. \end{aligned} \quad (\text{B1})$$

Finally, if two probability distributions p_A and p_B originate from measurements $\{M_i\}_i$ and $\{N_j\}_j$ on two independent quantum states ρ and σ , respectively, then the joint measurement $\{M_i \otimes N_j\}_{ij}$ acting on $\rho \otimes \sigma$ generates probability $p_A \otimes p_B$.

Appendix C: Causality description in GPTs

In classical causal theories formalized as Bayesian networks, all the causal influences are modelled as conditional probabilities between random variables. In quantum causal theories, causal influences between solely observed variables are the same as Bayesian networks. Differently, the causal influence from a latent variable on an observed variable X is characterized as a quantum instrument [44, 45]. The latent variable provides an input state, ρ , to the quantum instrument. The quantum instrument takes a measurement on ρ , which is characterized as a POVM $\{M_x\}_x$, and outputs the measurement outcome X . The causal influence from ρ to X is reflected from the outcome probability, where $X = x$ is output with probability $p(x) = \text{tr}(\rho M_x)$. With respect to the measurement outcome x , the quantum instrument also outputs a post-measurement system in the state $E_x \rho E_x^\dagger / \text{tr}(\rho E_x^\dagger E_x)$, where E_x is called a Kraus operator, satisfying $E_x^\dagger E_x = M_x$. Besides the latent vari-

able, if the observed variable X is also influenced by another observed variable A , A acts as a classical control, such that $p(X = x|A = a) = \text{tr}(\rho M_x^a)$, where each value of $A = a$ corresponds to a quantum instrument with POVM $\{M_x^a\}_x$.

To unify the descriptions of classical and quantum causal theories and generalize them to more relaxed physical theories within the GPT framework, we take advantage of the generalized operational-probabilistic framework [18]. The description is not directly applicable to the causal DAGs. For this purpose, we further apply the graphical interpretation introduced by Henson *et al.* [25].

We first review the generalized operational-probabilistic framework, which provides a unified framework to describe general physical operations in various theories. Above all, the generalized operational-probabilistic framework explicitly distinguishes observed classical variables from the system states underlying the physical processes. The first part of the framework is the definition of operations. A general physical operation is called a “test”, which generalizes the concept of quantum instrument in quantum information. The input system of the test carries a physical state in the underlying GPT. After measuring the state, the test outputs a classical variable as the measurement outcome. In addition, the test also outputs an associated post-measurement system.

After specifying operations, the framework describes the measurement outcomes in a probabilistic manner, which is consistent with the GPT assumptions in Box 1. In general, the measurement outcome is a random variable with more than one possible values, corresponding to the concept of “events” in probability theory. When two tests lead to the same probability distribution over the same set of events, and the replacement of one test with another does not affect the input and output systems, they are said to have the same “effect”. If the measurement outcome can take only one possible value, the test is called deterministic. For GPTs subjected to the assumptions in Box, we have the following result.

Lemma 3 (Uniqueness of the deterministic effect [18]). *For every system in a GPT, there exists a unique deterministic effect.*

Intuitively, the deterministic effect refers to discarding the system and ignoring the measurement outcome. As we will show later, this property is important to properly define the marginal distribution.

The operational-probabilistic framework is not automatically adaptable to the causal description in terms of the observed probability distribution in DAGs. We need to properly interpret the physical meanings of vertices and edges to describe the observed probability distribution in the causal DAG self-consistently. In particular, we hope the description is consistent with the d-separation criteria for Bayesian networks. For this purpose, we utilize the interpretation introduced by Henson *et al.* [25]. Under this interpretation, each vertex in the DAG, to-

gether with its incoming and outgoing edges, is described as a test, where the vertex loads the measurement outcome, the incoming edges load the input systems, and the outgoing edges load the output systems. If a vertex corresponds to an observed variable, we take it as a test with a non-trivial measurement outcome but a trivial output system; namely, only the measurement outcome is recorded, and the post-measurement system is discarded. If a vertex corresponds to a latent variable, we take it as a test with an output system in a non-trivial GPT state but a trivial measurement outcome. Following the same notation convention as Henson *et al.* [25], for completeness we assign a fixed value $\Lambda \equiv 1$ to a latent variable Λ ; hence every vertex in a causal DAG is assigned with a classical variable.

For vertex v , denote its parental vertices as $\text{pa}(v)$, the joint system of its incoming edges as $\text{inc}(v)$, and the joint system of its outgoing edges as $\text{out}(v)$. To describe the causal influences from $\text{pa}(v)$ on v , we record both the variable values of the vertices and the physical systems in a function

$$\mathcal{T}(X_v|X_{\text{pa}(v)})_{\text{out}(v)}^{\text{inc}(v)} : \mathcal{X}_v \times \mathcal{X}_{\text{pa}(v)} \rightarrow \mathbb{R}, \quad (\text{C1})$$

where X_v and $X_{\text{pa}(v)}$ represent the associated variables of v and $\text{pa}(v)$, \mathcal{X}_v and $\mathcal{X}_{\text{pa}(v)}$ represent their event spaces, and $\text{inc}(v)$ and $\text{out}(v)$ represent the incoming and outgoing systems of the test, respectively. Note that $X_{\text{pa}(v)}$ might be a joint random variable that corresponds to multiple vertices. In addition, if v is a root vertex such that $\text{pa}(v) = \emptyset, \text{inc}(v) = \emptyset$, we may write the function simply as $\mathcal{T}(X_v)_{\text{out}(v)}$. According to the GPT formulation, the above function can be taken as a probability kernel over X_v given $X_{\text{pa}(v)}$. To see this,

1. When v corresponds to an unobserved variable, we take its associating variable X_v as a variable with a definite value. This trivially satisfies the probability kernel definition in Eq. (1).
2. When v corresponds to an observed variable, $\text{out}(v)$ is a trivial output system. For any fixed value of $X_{\text{pa}(v)} = x_{\text{pa}(v)}$, the summation

$$\sum_{X_v=x_v} \mathcal{T}(x_v|x_{\text{pa}(v)})_{\text{out}(v)}^{\text{inc}(v)} \quad (\text{C2})$$

is equivalent to applying a deterministic effect to the composite system $\text{inc}(v)$, mapping the quantity to identity. According to Lemma 3, this map is unique. Therefore, $\mathcal{T}(x_v|x_{\text{pa}(v)})_{\text{out}(v)}^{\text{inc}(v)}$ satisfies the probability kernel definition in Eq. (1).

Note that the kernel function calculation depends on the underlying input system $\text{inc}(v)$ and the output system $\text{out}(v)$. If the incoming or the outgoing system is trivial, we omit the corresponding notation. If the parental and child vertices both correspond to observed variables, $\text{inc}(v)$ and $\text{out}(v)$ become trivial systems, and

$\mathcal{T}(X_v|X_{\text{pa}(v)})_{\text{out}(v)}^{\text{inc}(v)}$ degenerates to the usual conditional probability of X_v given $X_{\text{pa}(v)}$. For simplicity, we use the usual probability notations in this case. In addition, if a vertex is childless, we can determine the marginal distribution for the variables of other vertices by replacing this childless vertex with the deterministic effect. For a given probability kernel, the uniqueness of the deterministic effect guarantees the uniqueness of the marginal distribution [18, 25]. In later discussions, we sometimes use names of vertices and their corresponding variables interchangeably for brevity.

The above GPT causality formulation generalizes the Markov condition in a classical Bayesian network. Given a causal DAG G with m vertices X_1, \dots, X_m , where the first n vertices X_1, \dots, X_n correspond to observed variables. A probability kernel p over the observed variables is said to be generalized Markov with respect to G in a GPT if there exists a decomposition of

$$p(X_1 = x_1, \dots, X_n = x_n) = \prod_{i=1}^m \mathcal{T}(x_i|x_{\text{pa}_G(X_i)})_{\text{out}(X_i)}^{\text{inc}(X_i)}, \quad (\text{C3})$$

where the function \mathcal{T} is defined by the physical rules in the GPT. For instance, in Fig. 2(a), we have

$$\begin{aligned} & p(X = x, A = a, B = b, C = c, \Lambda = 1) \\ &= p(x)\mathcal{T}(a|x)^{\mathcal{H}_A}p(b|a)\mathcal{T}(c|b)^{\mathcal{H}_C}\mathcal{T}(\Lambda = 1)_{\mathcal{H}_{AC}}. \end{aligned} \quad (\text{C4})$$

Note that the term $\mathcal{T}(a|x)^{\mathcal{H}_A}, \mathcal{T}(c|b)^{\mathcal{H}_C}, \mathcal{T}(\Lambda = 1)_{\mathcal{H}_{AC}}$ are not independent of each other, as is reflected from the dependence on the non-trivial incoming or outgoing systems. Here, the trivial classical variable $\Lambda \equiv 1$ is assigned to the vertex of the latent variable, and we borrow the notation for Hilbert spaces in quantum theory to denote the systems, which are \mathcal{H}_{AC} for the output system of Λ , \mathcal{H}_A for the input system of A , and \mathcal{H}_C for the input system of C . The probability kernel decomposition captures the essence of the Markov condition, where the probability distribution of each vertex is only directly influenced by its parental vertices. Thus, we say $p(X, A, B, C, \Lambda)$ is generalized Markov.

In classical Bayesian networks, the conditional independences among observed variables are equivalent to the graphical criteria of d-separation [5]. Namely, two observed variables X_i and X_j are independent conditioned on a set of variables X_{k_1}, \dots, X_{k_m} if and only if the corresponding vertices of X_i and X_j are d-separated by the set of vertices corresponding to X_{k_1}, \dots, X_{k_m} . For convenience of later discussions, we briefly review the d-separation criteria here. Consider a DAG with vertices $\mathcal{V} := \{v_1, \dots, v_n\}$. We say that two vertices v_i, v_j are d-separated by a set of vertices $\mathcal{W} \subseteq \mathcal{V} \setminus \{v_i, v_j\}$ (\mathcal{W} can be an empty set) if for any path $v_i =: v_{k_1}, \dots, v_{k_m} =: v_j$ that links v_i and v_j in G , it holds that

1. If there are ‘‘colliders’’ in the path, namely, the kind of vertex $v_{k_{m'}}$ such that both $v_{k_{m'-1}}$ and $v_{k_{m'+1}}$ are connected to $v_{k_{m'}}$ through an edge pointing towards $v_{k_{m'}}$, i.e., $v_{k_{m'-1}} \rightarrow v_{k_{m'}} \leftarrow v_{k_{m'+1}}$, it holds

that there exists at least one collider that both the collider itself and its descendants do not belong to \mathcal{W} ;

2. Denoting \mathcal{V}' as the set of vertices that are non-colliders in the path other than v_{k_1} and v_{k_m} , then we have that either $\mathcal{V}' = \emptyset$ or $\mathcal{V}' \cap \mathcal{W} \neq \emptyset$.

A remarkable property of the generalized Markov condition is that it preserves the equivalence between (conditional) independences and (conditional) d-separation in GPTs [25]. For instance, in Fig. 2(a), as the causal influence of X on B is mediated by A , we have the independence condition of $X \perp\!\!\!\perp B|A$ shown by the following kernel decomposition:

$$\begin{aligned} p(x, a, b) &= \sum_{C=c} p(X = x, A = a, B = b, C = c) \\ &= p(x)\mathcal{T}(a|x)^{\mathcal{H}_A}p(b|a). \end{aligned} \quad (\text{C5})$$

The marginalization over C is valid since it is childless in the DAG. Graphically, the conditional independence can be shown by blocking the node A in the original directed path of $X \rightarrow A \rightarrow B$, the conditional d-separation criterion.

Appendix D: Nested Markov property in GPTs

In this section, we prove Theorem 1. Before moving on to the proof, we remark that we only study causal structures without vertices of nonexogenous unobserved variables [33]. Namely, all the vertices of latent variables are root vertices in the DAGs. Otherwise, the nested Markov model is not well-defined [7, 26]. There exist some discussions on a fully quantum causal theory, allowing vertices of latent variables to have both a non-trivial incoming and an outgoing system [33, 46, 47]. We refer readers interested in this topic to these references and cited results therein.

The nested Markov model is specified by equality constraints among observed variables, including the usual conditional independences and Verma constraints. In Evans [7], it has been proven that these equality constraints enumerate all of those in a Bayesian network with latent variables. Here, we show that these equality constraints remain valid when the latent variables are generalized to physical states in a GPT subjected to assumptions in Box 1. Note that the usual conditional independence, which is graphically equivalent to the d-separation, has been proven to hold in GPTs [25]. It thus remains to prove the validity of Verma constraints in GPTs.

To prove the statement, we shall take a graph-based approach. Before we commence, we first introduce the graphical tools. Consider a DAG G and an underlying GPT. The vertices of G include both observed and latent vertices. We divide all the vertices into two disjoint sets V and W . This partition can be arbitrary, depending

on the choice of probability queries used in the analysis. We call the ones in W as “fixed vertices”, which correspond to the random variables that are conditioned on in the probability queries of interest. Analogously, we call the ones in V as “random vertices”, which correspond to the random variables that are not appeared in the conditioning set. Throughout this paper, we require that the vertices in the “fixed vertex set” W must be parentless and their associated variables must be observed. Furthermore, we partition V into the set of observed vertices $V_{\mathcal{O}}$ and the set of unobserved vertices $V_{\mathcal{U}}$. Denote the edge set of G as \mathcal{E} , where every edge is directed from a vertex to another one. Then, the associated mDAG of G is defined as follows.

Definition 4 (mDAG and subgraph, Definition 2.6 of Evans [7]). *The associated mDAG of $G(V, W, \mathcal{E})$ is a hyper-graph $G(V_{\mathcal{O}}, W, \mathcal{E}_{\{V_{\mathcal{O}}, W\}}, \mathcal{B})$, where $\mathcal{E}_{\{V_{\mathcal{O}}, W\}}$ is the set of directed edges restricted to the vertices of observed variables $V_{\mathcal{O}}$ and fixed vertices W , and \mathcal{B} is an abstract simplicial complex over $V_{\mathcal{O}}$. An mDAG $G'(V', W', \mathcal{E}', \mathcal{B}')$ is a subgraph of $G(V_{\mathcal{O}}, W, \mathcal{E}_{\{V_{\mathcal{O}}, W\}}, \mathcal{B})$ if $V' \subseteq V_{\mathcal{O}}, W' \subseteq V_{\mathcal{O}} \cup W, \mathcal{E}' \subseteq \mathcal{E}_{\{V_{\mathcal{O}}, W\}}, \mathcal{B}' \subseteq \mathcal{B}$.*

Here, an abstract simplicial complex \mathcal{B} over $V_{\mathcal{O}}$ is a set of sets of vertices in $V_{\mathcal{O}}$, where (1) every single vertex set $\{v\} \in \mathcal{B}$, and (2) if $\mathcal{S} \in \mathcal{B}$ and $\mathcal{R} \subseteq \mathcal{S}, \mathcal{R} \neq \emptyset$, then $\mathcal{R} \in \mathcal{B}$. All the vertices in a generalized mDAG correspond to observed variables. With respect to the original DAG, a non-trivial maximal set in \mathcal{B} , or a bi-directed face, corresponds to the inclusion maximal set of observed vertices that are linked to a single latent vertex. Graphically, we obtain an associated mDAG of a causal DAG by taking the following procedure [26]: First, remove all the latent vertices in the DAG of the causal structure. Then, to reflect the influences of the latent variables on the observed variables in the mDAG, add a bi-directed edge between every two observed variables that are influenced by the same latent variable.

With respect to the abstract simplicial complex \mathcal{B} , we can partition the random vertices of an mDAG into districts, which are sets of vertices D_k that are mutually disjoint. The partition is derived as follows. First, label the set of random vertices V in an mDAG $G(V, W, \mathcal{E}, \mathcal{B})$ with an index set \mathcal{I} . From $i = 1$ to $|\mathcal{I}|$, if v_i is not already in a district,

1. If v_i is not bi-directed with any other ones, define a district as the single vertex $\{v_i\}$;
2. Otherwise, find the inclusion maximal set of random vertices v_{k_1}, \dots, v_{k_l} where $v_{k_1} = v_i$, and for every adjacent pair of vertices with labels $k_t, k_{t+1} \in \mathcal{I}$, $\{v_{k_t}, v_{k_{t+1}}\} \in \mathcal{B}$; define a district as this set of vertices.

Given a district D_k in an mDAG G , we define its associated subgraph $G[D_k]$ of G as follows: $G[D_k]$ contains vertices in D_k and their parental vertices, $\text{pa}_G(D_k) \setminus D_k$, which takes D_k as random and $\text{pa}_G(D_k) \setminus D_k$ as fixed; the

edges of $G[D_k]$ are naturally inherited from the original mDAG G , including the directed and bi-directed edges. There are three types of a district’s associated subgraph:

1. A single vertex: there is not a directed edge or a bi-directed edge in the subgraph;
2. DAG-type subgraph: the subgraph contains directed edges directing from fixed parental vertices to random child vertices, but it does not contain a bi-directed edge;
3. mDAG-type subgraph: the subgraph contains both directed edges and bi-directed edges, with fixed vertices the parents and random vertices the children.

Observation 1. *Note that in defining a subgraph, we first specify random vertices. For this reason, we have the following observations.*

1. In the DAG-type subgraph, each fixed vertex has a single random child vertex. Otherwise, the set of free vertices can be further divided into smaller districts.
2. In the mDAG-type subgraph, it is possible that free vertices linked by bi-directed edges have no parental vertices.

In the study of Bayesian networks, a graphically recursive procedure was proposed to find Verma constraints [6], which is based on the notion of nested Markov property.

Definition 5 (Nested Markov property, Definition 3.1 in Evans [7]). *Given an mDAG $G(V, W, \mathcal{E}, \mathcal{B})$, suppose a distribution p defines a valid probability kernel over the state space of V , namely \mathcal{X}_V , indexed by \mathcal{X}_W . Then, it obeys the nested Markov property with respect to $G(V, W, \mathcal{E}, \mathcal{B})$ if $V = \emptyset$, or both*

1. p can be factorized over districts D_1, \dots, D_l of G :

$$p(x_v | x_w) = \prod_{i=1}^l g_i(x_{D_i} | x_{\text{pa}(D_i) \setminus D_i}), \quad (\text{D1})$$

where every g_i is a probability kernel obeying the nested Markov property with respect to the subgraph $G[D_i]$ if $l \geq 2$ or $W \setminus \text{pa}_G(V) \neq \emptyset$,

2. $\forall v \in V$ such that $\text{ch}_G(v) = \emptyset$, the marginal kernel over the state space of $V \setminus v$ indexed by \mathcal{X}_W

$$p(x_{V \setminus v} | x_w) = \sum_{x_v} p(x_v | x_w) \quad (\text{D2})$$

obeys the nested Markov property with respect to the subgraph $G[V \setminus \{v\}]$.

In Tian and Pearl [6], Evans [7], it was proved that given a causal DAG $G(V, W, \mathcal{E})$, if a probability kernel p over \mathcal{X}_V indexed by \mathcal{X}_W can be generated from G when G is considered as a Bayesian network, then p enjoys

the nested Markov property with respect to the mDAG associated with $G(V, W, \mathcal{E})$. Note that Eq. (D2) defines the nested Markov property in a recursive manner, which naturally defines the procedure to search for Verma constraints: After the marginalization over a childless free vertex v in Eq. (D2), for the resulted subgraph and its associated probability kernel, repeat the two steps in Eq. (D1) and (D2). Note that an mDAG might contain multiple childless free vertices, and we need to marginalize each of them and apply the same procedure to each resulted subgraph separately. The procedure ends for a subgraph if it contains a single random vertex. In the marginalization step of Eq. (D2), if we find the marginal kernel, $\sum_{x_v} p(x_V | x_W)$, is independent of the variable values of a strict subset of the fixed vertices, $W' \subsetneq W$, then we find a Verma constraint similar to Eq. (5).

In Evans [7], the author further proved that the recursive procedure enumerates exactly all the Verma constraints in a Bayesian network. In other words, the recursive procedure is an equivalent definition for the nested Markov model. In our results, we generalize this statement to GPTs. Specifically, when the latent variables in the causal DAG G are characterized as GPT physical states satisfying assumptions in Box 1, every probability kernel that can be generated from G obeys the nested Markov property with respect to G .

To prove the result, we shall show that each step of the recursive procedure results in a valid probability kernel that is consistent with the subgraph. To start the proof, consider a generalized DAG G with m vertices, where the first n vertices are observed, and a probability distribution p over the variables of observed vertices that is generalized Markov with respect to G within some GPT, given by

$$p(X_1 = x_1, \dots, X_n = x_n) = \prod_{i=1}^m \mathcal{T}(x_i | x_{\text{pa}(i)})_{\text{out}(i)}^{\text{inc}(i)}. \quad (\text{D3})$$

Note that in the causal DAGs we consider, a test underlying a vertex has at most a non-trivial incoming or outgoing system; the notation $\mathcal{T}(x_i | x_{\text{pa}(i)})_{\text{out}(i)}^{\text{inc}(i)}$ is merely for the convenience of statements. To avoid heavy notations, when multiple vertices are mentioned with a necessity of a label set, we represent a vertex simply by its label i and use X_i to represent its corresponding variable. In addition, $X_{\text{pa}(i)}$ is abbreviated for the variables corresponding to the parental vertices of the i 'th vertex. If only a single general vertex is mentioned, we use v to represent it.

At the beginning, we take all the observed vertices in the DAG G and hence all the vertices in its associated mDAG as random, i.e., X_1, \dots, X_n . Suppose these vertices can be partitioned into districts D_1, \dots, D_k , and the abstract simplicial complex of mDAG is \mathcal{B} . We first show that it is valid to factorize the distribution p over the districts and obtain the factorized distributions for the associated subgraphs. We discuss the issue for each type of subgraphs separately.

Lemma 4. *If a subgraph $G[D_j]$ does not have bi-directed edges, then the marginal distribution of p over $G[D_j]$ can be equivalently described by a probability kernel of a Bayesian network.*

Proof. First, we explain that the subgraph $G[D_j]$ has well-defined operational-probabilistic descriptions.

1. For the case of a single vertex v , in the original generalized DAG, it does not have a parent vertex, hence the input system to its underlying test is trivial. The vertex can thus be equivalently described by a random variable with distribution $p(x_v)$.
2. For the case of a DAG-type subgraph, consider an end vertex v , where $\text{ch}_G(v) = \emptyset$. Since it only has observed parental vertices in G , the input system to its underlying test is trivial. Since the parental vertices of v are fixed in the subgraph, for every value of its observed parent nodes $x_{\text{pa}(v)}$, the probability kernel over \mathcal{X}_v indexed by $\mathcal{X}_{\text{pa}(v)}$ can be equivalently described by a random variable with distribution $p(x_v | x_{\text{pa}(v)})$.

Second, we argue that describing $p(x_v | x_{\text{pa}(v)})$ as equivalently obtained from a Bayesian network is valid. Consider a Bayesian network G' with the same vertex and edge sets as $G[D_j]$. According to Theorem 2 in Evans [26], the set of valid distributions of $G[D_j]$ and G' are the same. Therefore, any valid p can be obtained in G' . In addition, since the free vertices correspond to observed variables, they have a trivial output system in the corresponding tests. Since both the input and output systems of these tests are trivial, replacing these tests with equivalent effects does not make a difference in the probability kernel over other districts. \square

Lemma 5. *Consider a subgraph $G[D_j]$, where vertices in the district D_j contain non-trivial maximal sets $B_1, \dots, B_l \in \mathcal{B}$, which correspond to latent variables X_{n+1}, \dots, X_{n+l} in the original DAG G . In addition, partition the parental vertices of a vertex $i \in D_j$ in G into the ones corresponding to observed and latent variables and denote the observed ones as $\text{opa}(i)$. Then, the probability kernel over D_j given the variables of its observed parental vertices $\text{opa}(D_j)$ is given by*

$$\prod_{i \in D_j} \mathcal{T}(x_i | x_{\text{opa}(i)})_{\text{out}(i)}^{\text{inc}(i)} \prod_{i'=1}^l \mathcal{T}(X_{n+i'} = 1)_{\text{out}(n+i')}. \quad (\text{D4})$$

Proof. We argue that in the above expression, the state of a non-trivial outgoing system $\text{out}(n+i')$ is not an input system to the tests of vertices that are outside D_j . Otherwise, the set $B_{i'}$ is not a maximal set in \mathcal{B} , which disagrees with the definition of the district. In addition, all the input systems of the random vertices $\text{inc}(i)$ match a (sub-) output system of the latent vertices $\text{out}(n+i')$ in this district by definition. Therefore, the above expression can be separated from the probability kernel p without affecting the effects on other vertices. Then, it can

be directly checked that this expression is a non-negative function over $\mathcal{X}_{D_j} \times \mathcal{X}_{\text{opa}(D_j)}$, and the summation over all possible values of X_{D_j} leads to identity. \square

In summary, given a generalized DAG G and a GPT, starting from a valid probability distribution in Eq. (D3) that is generalized Markov with respect to G ,

1. Lemma 4 allows an equivalent replacement of the “classical part” in the graph, namely the subgraph that does not contain a bi-directed edge, with a usual probability distribution;
2. Lemma 5 shows that the “GPT part” in the graph, namely the subgraphs that contain bi-directed simplicial complexes, define a valid probability kernels that can be separated from the entire probability.

While we analyse Lemma 4 and 5 on the initial mDAG associated with the original causal DAG, the results naturally extend to a general mDAG, which may contain a non-empty set of fixed vertices. By this, we prove the validity of Eq. (D1) in GPTs. Based on this, we arrive at the following theorem.

Theorem 3 (Nested Markov property in GPTs). *Given a causal DAG G and a GPT, suppose a probability distribution p over the observed vertices is generalized Markov with respect to G , as defined in Eq. (D3). Then, the distribution p satisfies the nested Markov property in terms of the graphical recursive procedure through Eq. (D1) to (D2).*

Proof. Lemma 4 and 5 define a recursive procedure that reduces some random vertices or the overall graph size (containing both random and fixed vertices). We mainly need to check Eq. (D2), namely, the margins of the kernels define a kernel that allows the application of the recursive procedure.

1. For the “classical parts” discussed in Lemma 4, they satisfy the usual nested Markov property for a Bayesian network.
2. For the “GPT parts” discussed in Lemma 5, a childless random vertex must be connected to other random vertices by bi-directed edges; otherwise, it degenerates to a “classical” case. For the probability kernel of a general mDAG-type subgraph in Eq. (D4), a childless random vertex t can be further divided into two types:

- (a) The vertex t is only linked by one bi-directed edge, which corresponds to the latent variable $X_{n+t'}$. After marginalizing X_t of vertex t in the proba-

bility kernel, we have the expression

$$\begin{aligned}
& \sum_{X_t=x_t} \prod_{i \in D_j} \mathcal{T}(x_i | x_{\text{opa}(i)})^{\text{inc}(i)} \prod_{i'=1}^l \mathcal{T}(X_{n+i'} = 1)_{\text{out}(n+i')} \\
&= \prod_{i \in D_j, i \neq t} \mathcal{T}(x_i | x_{\text{opa}(i)})^{\text{inc}(i)} \prod_{i'=1}^l \mathcal{T}(X_{n+i'} = 1)_{\text{out}(n+i')} \\
&= \prod_{i \in D_j, i \neq t} \mathcal{T}(x_i | x_{\text{opa}(i)})^{\text{inc}(i)} \prod_{i'=1, i' \neq t'}^l \mathcal{T}(X_{n+i'} = 1)_{\text{out}(n+i')} \\
& \quad \times \mathcal{T}(X_{n+t'} = 1)_{\text{out}(n+t') \setminus \text{inc}(t)},
\end{aligned} \tag{D5}$$

where $\text{out}(n+t') \setminus \text{inc}(t)$ represents the joint system modulo the input system to the test of X_t , $\text{inc}(t)$. Additionally, this expression removes the observed parent vertices of t that are not parental to other random vertices. Similar to the arguments in the proof of Lemma 5, the above expression is a valid probability kernel, and the non-trivial input and output systems in the decomposition are not shared by a probability kernel outside the district after marginalization. That is, the probability kernel after marginalization is consistent with resulted subgraph.

- (b) The vertex is linked by multiple bi-directed edges. We discuss the case corresponding to two latent variables X_{n+t_1}, X_{n+t_2} , and the cases for more latent variables can be analysed similarly. After marginalizing X_t in the probability kernel, we have the expression

$$\begin{aligned}
& \sum_{X_t=x_t} \prod_{i \in D_j} \mathcal{T}(x_i | x_{\text{opa}(i)})^{\text{inc}(i)} \prod_{i'=1}^l \mathcal{T}(X_{n+i'} = 1)_{\text{out}(n+i')} \\
&= \prod_{i \in D_j, i \neq t} \mathcal{T}(x_i | x_{\text{opa}(i)})^{\text{inc}(i)} \prod_{i'=1}^l \mathcal{T}(X_{n+i'} = 1)_{\text{out}(n+i')} \\
&= \prod_{i \in B_{t_1}, i \neq t} \mathcal{T}(x_i | x_{\text{opa}(i)})^{\text{inc}(i)} \mathcal{T}(X_{n+t_1} = 1)_{\text{out}(n+t_1) \setminus \text{inc}(t)} \\
& \quad \times \prod_{i \in B_{t_2}, i \neq t} \mathcal{T}(x_i | x_{\text{opa}(i)})^{\text{inc}(i)} \mathcal{T}(X_{n+t_2} = 1)_{\text{out}(n+t_2) \setminus \text{inc}(t)} \\
& \quad \times \prod_{i'=1, i' \neq t_1, t_2}^l \mathcal{T}(X_{n+i'} = 1)_{\text{out}(n+i')}.
\end{aligned} \tag{D6}$$

In the second equality, the non-trivial output systems $\text{out}(n+t_1) \setminus \text{inc}(t)$ are embedded in some subsystems of $\text{inc}(i)$ with $i \in B_{t_1}, i \neq t$; the non-trivial output systems $\text{out}(n+t_2) \setminus \text{inc}(t)$ are embedded in some subsystems $\text{inc}(i)$ with $i \in B_{t_2}, i \neq t$; and the non-trivial output systems $\text{out}(n+i')$ for $i' \neq t_1, t_2$ match the rest of the non-trivial input subsystems. Then, it can be directly checked

that the above expression is a valid probability kernel consistent with the subgraph.

Therefore, we have checked that the procedure in defining the nested Markov property hold valid in GPTs. \square

Appendix E: Comparison between the nested Markov model and GPTs

In this section, we prove the results in Sec. IV, which is about understanding the relationships between the nested Markov model, GPTs and our new causal model.

1. Proof of Proposition 1

Proof. Given a general causal graph G , by construction, every vertex in the hypergraph $H(G)$ is either a root or an end vertex. Let us partition the vertices of observed variables into districts and consider the associated mDAG of $H(G)$. To prove the proposition, we show that in the procedure through Eq. (D1) to Eq. (D2), the conditional independences are already reflected from the d-separation in the initial graph $H(G)$.

First, consider a subgraph that does not contain bi-directed edges. The underlying district is defined by a single random vertex v , and its associated subgraph contains v as a random vertex and $\text{pa}_{H(G)}(v)$ as fixed vertices. The conditional independence of v from $H(G) \setminus \{v, \text{pa}_{H(G)}(v)\}$ can be determined by applying the d-separation to $H(G)$. Since v is an end vertex, after applying Eq. (D2), we obtain a trivial probability kernel of unity. Therefore, the recursive procedure defining the nested Markov model ends in this subgraph.

Next, consider a subgraph defined by a non-trivial district D , where the vertices v_1, \dots, v_n in the district are joined by bi-directed edges. Note that there might be several bi-directed edges. In the subgraph, the free vertices, which are childless, can be categorized into the following types (see an example in Fig. 5, where A, B, C, D , and E define a district involving bi-directed edges): (1) the vertex does not have an observed parental vertex, and it is linked to other free vertices by one bi-directed edge (e.g., vertex E); (2) the vertex has an observed parental vertex, and it is linked to other free vertices by one bi-directed edge (e.g., vertex A); (3) the vertex does not have observed parental vertices, and it is linked to other free vertices by more than one bi-directed edges (e.g., vertices B and D); and (4) the vertex has observed parental vertices, and it is linked to other free vertices by several bi-directed edges (e.g., vertex C).

1. For vertices of type (1), a marginalization over them results in a trivial probability kernel of unity.
2. For a vertex v of type (2), suppose its fixed vertices $\text{pa}_{H(G)}(v)$ can be divided into disjoint vertex sets W_1 and W_2 , where W_1 are all the vertices that

are not the parental vertices of other random vertices. Then, a marginalization over the variable of v in the probability kernel manifests an independence between the variables of fixed vertices, W_1 , and the subgraph $H(G) \setminus \{v, W_1\}$. Nevertheless, since any sequence of edges linking W_1 and $H(G) \setminus \{v, W_1\}$ must go through the vertex v , which is a collider in the sequence, the above independence can be determined by applying the d-separation to $H(G)$.

3. For a vertex v of type (3), without loss of generality, suppose it is linked to other random variables by a bi-directed edge representing the latent variable Λ_1 and a bi-directed edge representing the latent variable Λ_2 in the causal DAG of $H(G)$. A marginalization over the variable of v results in a trivial probability kernel of unity. If there is not another common child vertex of Λ_1 and Λ_2 in $H(G)$, then the marginalization results in a decomposition of two independent probability kernels, which originate from Λ_1 and Λ_2 , respectively. Nevertheless, since v is a collider between Λ_1 and Λ_2 , the independence between the kernels can be determined by applying the d-separation to $H(G)$.
4. For a vertex v of type (4), by combining the analysis for types (2) and (3), one can see that there is not an independence that is absent in usual conditional independence in the DAG $H(G)$.

\square

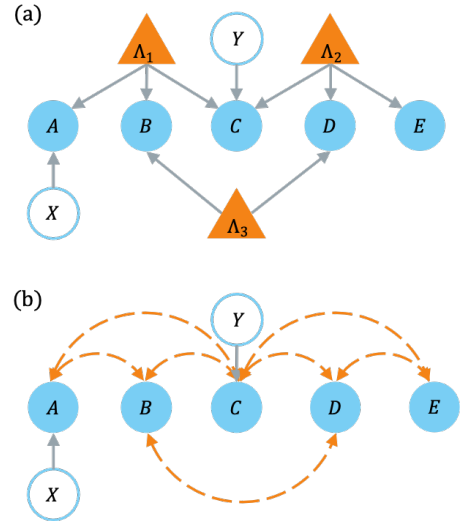


FIG. 5. (a) An example causal DAG of $H(G)$. The DAG contains vertices of observed variables, X, Y, A, B, C, D, E , and vertices of latent variables, $\Lambda_1, \Lambda_2, \Lambda_3$. Initially taking all the random vertices as free, the free vertices can be divided into three districts: $\{X\}$, $\{Y\}$, and $\{A, B, C, D, E\}$. For the district containing bi-directed edges. (b) The associated mDAG of $H(G)$.

2. Proof of Proposition 2

Proof. Consider a causal DAG $G(V, W, \mathcal{E})$ as described in Def. 1, which has N vertices in total and n vertices corresponding to observed variables. Its associated Bell-type hypergraph $H(G)(V \cup U, W, \mathcal{E}')$ is defined as in Def. 2. In addition, consider a specific GPT \mathcal{G} that satisfies the assumptions in Box 1.

Part 1: $\mathcal{G}(G) \subseteq P(\mathcal{G}(H(G)))$

Suppose a probability distribution p among observed variables of V in G can be generated within \mathcal{G} and admits a generalized Markov decomposition:

$$p(x_1, \dots, x_n) = \prod_{i=1}^N \mathcal{T}(x_i | x_{\text{pa}_G(i)})_{\text{out}(i)}^{\text{inc}(i)}. \quad (\text{E1})$$

For brevity, we abbreviate v_i as i in $\text{pa}_G(i), \text{inc}(i), \text{out}(i)$. We prove that there exists a valid probability distribution p' in $H(G)$ that can be generated within \mathcal{G} , such that $P(p') = p$, where P is the projection operation in Def. 2. To obtain such a distribution, we extend the distribution of p over G to $H(G)$ with respect to the operations in Def. 1. Consider an observed vertex $v_i \in V$ that has both incoming edges from $V \cup W$ and outgoing edges to other vertices in V . By definition, the vertex v_i is not a root vertex, and the terms that explicitly contain x_i in the kernel decomposition are given by

$$\mathcal{T}(x_i | x_{\text{pa}_G(i)})_{\text{out}(i)}^{\text{inc}(i)} \prod_{\substack{l: v_l \in V \\ v_l \in \text{pa}_G(i)}} \mathcal{T}(x_l | x_{\text{pa}_G(l)})_{\text{out}(l)}^{\text{inc}(l)}. \quad (\text{E2})$$

Here, we denote the number of v_l such that $v_l \in \text{pa}_G(i)$ as J_i . With respect to $H(G)$, we change the values of x_i to $x_{i,l}$ in the terms being conditioned in $\mathcal{T}(x_l | x_{\text{pa}_G(l)})_{\text{out}(l)}^{\text{inc}(l)}$:

$$\mathcal{T}(x_i | x_{\text{pa}_G(i)})_{\text{out}(i)}^{\text{inc}(i)} \prod_{l=1}^{J_i} \mathcal{T}(x_l | x_{\text{pa}_G(l) \setminus i}, x_{i,l})_{\text{out}(l)}^{\text{inc}(l)}, \quad (\text{E3})$$

where $x_{i,l}$ takes any value in the alphabet of X_i, \mathcal{X}_i . For each term of $\mathcal{T}(x_l | x_{\text{pa}_G(l) \setminus i}, x_{i,l})_{\text{out}(l)}^{\text{inc}(l)}$, since the incoming systems are not changed in the expression, hence the underlying physical states and classically controlled measurements for each fixed value remain the same as in Eq. (E2), i.e.,

$$\mathcal{T}(x_l | x_{\text{pa}_G(l)})_{\text{out}(l)}^{\text{inc}(l)} = \mathcal{T}(x_l | x_{\text{pa}_G(l) \setminus i}, x_{i,l})_{\text{out}(l)}^{\text{inc}(l)} \quad (\text{E4})$$

if $x_i = x_{i,l}$. Therefore, the following expression is a valid probability kernel:

$$\mathcal{T}(x_i | x_{\text{pa}_G(i)})_{\text{out}(i)}^{\text{inc}(i)} \prod_{l=1}^{J_i} \mathcal{T}(x_l | x_{\text{pa}_G(l) \setminus i}, x_{i,l})_{\text{out}(l)}^{\text{inc}(l)} p(x_{i,l}), \quad (\text{E5})$$

where $p(x_{i,l})$ is a probability distribution that is the same as $p(x_i)$. In addition, note that the outgoing systems of the latent variables in W that are parental vertices

of x_i, x_l are also not changed. Therefore, after applying the procedure to Eq. (E1) for every vertex that has both incoming edges from $V \cup W$ and outgoing edges to other vertices in V , we obtain a valid probability distribution p' over all the vertices of observed variables in $H(G)$. By construction, it satisfies the generalized Markov condition with respect to $H(G)$ within the GPT \mathcal{G} , and $P(p') = p$.

Part 2: $P(\mathcal{G}(H(G))) \subseteq \mathcal{G}(G)$

Suppose a probability distribution p' among observed variables of $V \cup U$ in $H(G)$ can be generated within \mathcal{G} and admits a generalized Markov decomposition:

$$p(x_1, \dots, x_n, x_{\ell_1,1}, \dots, x_{\ell_1, J_{\ell_1}}, \dots, x_{\ell_m,1}, \dots, x_{\ell_m, J_{\ell_m}}) \\ = \prod_{i=1}^N \mathcal{T}(x_i | x_{\text{pa}_{H(G)}(i)})_{\text{out}(i)}^{\text{inc}(i)} \prod_{j=1}^m \prod_{k=1}^{J_{\ell_j}} p(x_{\ell_j, k}). \quad (\text{E6})$$

We prove that $p \equiv P(p')$ is a valid probability distribution in G that can be generated within \mathcal{G} . Consider a set of vertices in U , $\{v_{i,1}, \dots, v_{i, J_i}\}$, where $v_{i,j}$ is the vertex added to the j 'th child vertex of $v_i \in V$, denoted as $v_{i,j} \in V$. In the rest part of the proof, we omit l for simplicity in the subscripts. By definition, the vertices $\{v_{i,1}, \dots, v_{i, J_i}\}$ are root vertices in $H(G)$, and the terms that explicitly contain $x_{i,1}$ in the kernel decomposition are given by

$$\prod_{j=1}^{J_i} p(x_{i,j}) \mathcal{T}(x_{i,j} | x_{i,j})_{\text{out}(i,j)}^{\text{inc}(i,j)}. \quad (\text{E7})$$

As a remark, each $x_{i,j}$ shows up once as the term being conditioned on. By taking the projection operation in Def. 2 and post-selecting the data of $x_{i,j} = x_i, \forall j$, the term $p(x_{i,j})$ is removed, and $\mathcal{T}(x_{i,j} | x_{i,j})_{\text{out}(i,j)}^{\text{inc}(i,j)}$ is set as $\mathcal{T}(x_{i,j} | x_i)_{\text{out}(i,j)}^{\text{inc}(i,j)}$. Similar to the argument in part 1, the non-trivial physical systems are not changed in the expression, and the resulted expression

$$\prod_{j=1}^{J_i} \mathcal{T}(x_{i,j} | x_i)_{\text{out}(i,j)}^{\text{inc}(i,j)} \quad (\text{E8})$$

is a valid probability kernel. Therefore, after applying the procedure to Eq. (E6) for each set of vertices in U that are added with respect to a vertex $v_i \in V$, we obtain a valid probability distribution $p = P(p')$ over all the vertices of observed variables in G . By construction, it satisfies the generalized Markov condition with respect to G . \square

3. Proof of Lemma 1

Proof. To show $\mathcal{GPT}(G) \subseteq \mathcal{PS}(G)$, because of Proposition 2, we simply need to check if $\mathcal{GPT}(H(G)) \subseteq$

$\mathcal{I}(H(G))$. This inclusion was proven in Henson *et al.* [25].

To show $\mathcal{PS}(G) \subseteq \mathcal{N}(G)$, we explain that for every probability distribution $p \in \mathcal{I}(H(G))$, the projected distribution $P(p)$ admits a factorization that respects the district decomposition in G and enjoys the nested Markov property with respect to G . For this purpose, we inspect the correspondence between the subgraphs of G and $H(G)$, and consequently their associated distributions. In the following, we refer to G and $H(G)$ as mDAGs, given by $G(V, W = \emptyset, \mathcal{E}, \mathcal{B})$ and $H(G)(V \cup U, W = \emptyset, \mathcal{E}', \mathcal{B}')$.

1. According to the construction of $H(G)$, we have $\mathcal{B} = \mathcal{B}'$. In other words, suppose the vertex set V of G can be decomposed into districts $\{D_i\}_{i=1}^t$. Then, the set of vertices in D_i also defines a district in $H(G)$. As $\bigcup_i D_i = V$, the district partition for $H(G)$ within the vertex set V is the same for G . In $H(G)$, all the supplemented vertices, namely those in the vertex set U , are root vertices, each of which has one single child vertex (see Observation 1). Therefore, each vertex $u_{l_j, k}$ defines a single-vertex district in $H(G)$.
2. Consider a probability distribution $p \in \mathcal{I}(H(G)) = \mathcal{N}(H(G))$. Then according to the nested Markov property in Def. 5, this distribution has a factorization with respect to the subgraphs:

$$p = \prod_{i=1}^t g_i(x_{D_i} | x_{\text{pa}_{H(G)}(D_i) \setminus D_i}) \prod_{j=1}^m \prod_{k=1}^{J_j} p(x_{l_j, k}), \quad (\text{E9})$$

where for the subgraph $H(G)[D_i]$, the conditional probability distribution is given by $g_i(x_{D_i} | x_{\text{pa}_{H(G)}(D_i) \setminus D_i})$. Furthermore, g_i obeys the nested Markov property with respect to the subgraph $H(G)[D_i]$. After the projection, the values of $x_{l_j, k}$ are fixed as $x_{l_j, k} \equiv x_{l_j}$; hence the terms $p(x_{l_j, k})$ are removed from the distribution factorization of $P(p)$, and we simply need to check the projected distribution $P(g_i)$. We argue that $P(g_i)$ obeys the nested Markov property with respect to the subgraph $G[D_i]$. We simply need to focus on the vertices in $\text{pa}_{H(G)}(D_i) \setminus D_i \cap U$ for this statement. Consider a general vertex of such, $u_{l_j, k}$, which originates from $v_{l_j, k} \in V$:

- (a) If $v_{l_j, k} \notin D_i$, then the projection operation, i.e., $x_{l_j, k} \equiv x_{l_j}$, does not change the conditional distribution g_i , merely with a renaming of the term being conditioned on without any change in the distribution.
- (b) If $v_{l_j, k} \in D_i$, then the projection operation removes the term $x_{l_j, k} \equiv x_{l_j}$ from the terms being conditioned in g_i .

For both cases, the projected distribution $P(g_i)$ is consistent with the division of free and fixed vertices in $G[D_i]$; hence it obeys the nested Markov property with

respect to $G[D_i]$. Note that $\mathcal{N}(G)$ is defined as that for every probability distribution $q \in \mathcal{N}(G)$, it can be factorized as

$$q = \prod_{i=1}^t h_i(x_{D_i} | x_{\text{pa}_{H(G)}(D_i) \setminus D_i}), \quad (\text{E10})$$

and each of h_i obeys the nested Markov property with respect to the subgraph $G[D_i]$. Comparing the factorization of $P(p)$ with respect to this form, we see that $P(p)$ admits a factorization with respect to G , i.e., in accordance with Eq. (D1) of Def. 5.

3. Finally, by construction, we naturally have that every childless vertex in G remains a childless vertex in $H(G)$. This shows that every variable associated with a childless vertex in G , which can be marginalized over in Eq. (D2) of Def. 5, can also be marginalized over in $H(G)$.

The above discussion shows that if $p \in \mathcal{I}(H(G))$, then $P(p)$ obeys the nested Markov property with respect to G . Putting everything together, we have $\mathcal{PS}(G) = \mathcal{P}(\mathcal{I}(H(G))) \subseteq \mathcal{N}(G)$. \square

4. Proof of Lemma 2

We prove the equality part of the lemma. The strict separation between $\mathcal{PS}(G)$ and $\mathcal{N}(G)$ is manifested in the discussion of Eq. (13).

Proof. To prove this statement, it suffices to prove that $\mathcal{GPT}(H(G)) = \mathcal{I}(H(G)) = \mathcal{NS}(H(G))$. Since G has only one latent variable, the hyper-graph $H(G)$ corresponds to a standard Bell test, where the number of non-local parties is equal to the number of child vertices of the latent variable in G . In $H(G)$, $\mathcal{GPT}(H(G)) \subseteq \mathcal{I}(H(G))$ holds, as the non-trivial requirements in $\mathcal{I}(H(G))$ correspond to non-signalling conditions, which should be satisfied by any valid GPT. Also, $\mathcal{I}(H(G)) = \mathcal{NS}(H(G))$, where $\mathcal{NS}(H(G))$ corresponds to the box-world, which is a valid GPT under assumptions in Box 1 [17, 20]. Since $\mathcal{NS}(H(G)) \subseteq \mathcal{GPT}(H(G))$, we have the equalities to hold. \square

5. Proof of Theorem 2

Previous sections plus Bell's theorem [15] show the inclusions in Eq. (16), and the existence of causal graphs with strict inclusions, $\mathcal{C}(G) \subsetneq \mathcal{GPT}(G)$, $\mathcal{PS}(G) \subsetneq \mathcal{N}(G)$, $\mathcal{N}(G) \subsetneq \mathcal{I}(G)$. In this section, we prove the remaining part, namely, the existence of causal graphs where $\mathcal{GPT}(G) \subsetneq \mathcal{PS}(G)$. We focus on Fig. 3(a) and prove that Eq. (14) cannot be generated within this structure in any GPT.

Proof. Consider the graph in Fig. 3(a) with all the observed vertices representing binary random variables, and a probability distribution $p(A, B, C, X, Z)$, where

$$\begin{aligned} \sum_a p(a, b, c|x, z) &\equiv p(b, c|z), \forall b, c, z \in \{0, 1\}, \\ \sum_b p(a, b, c|x, z) &\equiv p(a|x)p(c|z), \forall a, c, x, z \in \{0, 1\}, \\ \sum_c p(a, b, c|x, z) &\equiv p(a, b|x), \forall a, b, x \in \{0, 1\}, \\ p(a, b = 0, c|x, z) &= p(b = 0) \frac{1}{2} \delta_{a \oplus c = xz}. \end{aligned} \quad (\text{E11})$$

The first three equations guarantee that the probability distribution satisfies all the non-signalling constraints, hence $p \in \mathcal{I}(G)$. In addition, we have $\mathcal{PS}(G) = \mathcal{I}(G)$ by construction.

Suppose there is a GPT \mathcal{G} that can generate the probability distribution p . Then, the bipartite non-signalling probability distribution $q(A, C|X, Z)$ with

$$q(a, c|x, z) = \frac{1}{2} \delta_{a \oplus c = xz} \quad (\text{E12})$$

belongs to the set of valid states \mathcal{S} in this theory. This probability distribution is also called the standard Popescu-Rohrlich (PR) box [20]. In the GPT \mathcal{G} , the most general operations that act on this bipartite state allows the state to be transformed into a probability distribution [48]

$$\begin{aligned} q'(a, c|x, z) \\ = \begin{cases} \frac{1}{2}, & \text{if } a \oplus c = xz \oplus \alpha x \oplus \beta z \oplus \gamma, \\ 0, & \text{otherwise,} \end{cases} \end{aligned} \quad (\text{E13})$$

where $\alpha, \beta, \gamma = 0, 1$. We term these probabilities an (α, β, γ) -PR box, where the standard PR box corresponds to the case with $\alpha = \beta = \gamma = 0$. In addition, consider the set of allowed states on a single-party system. According to the convexity assumption for a valid GPT, any fixed input-output distribution should belong to the set of valid states. According to the parallel composition assumption, the tensor product of two such probabilities for a bipartite system represents a valid state. There are sixteen inequivalent states of such, which we denote as $p_{L_i}, i = 0, \dots, 15$.

By slightly modifying the results in Short *et al.* [31], we can prove that for Λ_1 and Λ_2 to be either an (α, β, γ) -PR box or a local distribution p_{L_i} , the model cannot generate the probability distribution p in Eq. (3). Using the results in Bierhorst [49] and the convexity assumption, any valid bipartite GPT state in \mathcal{G} with binary-valued observables can be decomposed into a convex combination of one (α, β, γ) -PR box and several p_{L_i} . Then, by using a convexity argument, which is consistent with the convexity assumption of the GPT, we arrive at the conclusion that \mathcal{G} cannot generate the probability distribution p in Eq. (3). \square

Appendix F: Common separation between classical and GPT causal models

In this section, we prove that Eq. (20) does not admit a causal explanation in a classical Bayesian network. To prove this result, first note that the set of probability distributions that can be generated from the causal DAG G of Fig. 4(a) within a GPT is convex, as there is only one latent variable. In particular, the set of distributions $\mathcal{C}(G)$ within a Bayesian network is a convex polytope. Therefore, we can list all extremal points of $\mathcal{C}(G)$. For this purpose, we take advantage of the projection technique in Def. 2. In the tripartite Bell test $H(G)$ of Fig. 4(b), when all the observed variables are binary, the set of probability distributions $\mathcal{C}(H(G))$ is spanned by the following extremal points:

$$p(a, b, c|x, y, z) = \begin{cases} 1, & a = \alpha x \oplus \beta, b = \gamma y \oplus \delta, c = \theta z + \eta, \\ 0, & \text{otherwise,} \end{cases} \quad (\text{F1})$$

where $\alpha, \beta, \gamma, \delta, \theta, \eta \in \{0, 1\}$. In total, there are $2^6 = 64$ extreme points in $\mathcal{C}(H(G))$. Next, we take the projection and obtain the extremal points in $\mathcal{C}(G)$ by taking $Y = A, Z = B$. Note that the projection results in some degeneracy. After the projection, the values of $A = a, B = b$, and $C = c$ are determined by

$$\begin{aligned} a &= \alpha x \oplus \beta, \\ b &= \gamma a \oplus \delta = \gamma(\alpha x \oplus \beta) \oplus \delta, \\ c &= \theta z + \eta = \theta(\gamma(\alpha x \oplus \beta) \oplus \delta) + \eta. \end{aligned} \quad (\text{F2})$$

We list the probability distributions in detail with respect to the values of a .

Case 1: When $\alpha = \beta = 0, b = \delta, c = \theta\delta \oplus \eta$, there is a deterministic output of $A = 0$. There are four extremal points in this case. We list the conditional probability distributions of $p(a, b, c|x)$ in Table II. A blank term in the table means that the conditional probability is zero.

Case 2: When $\alpha = 0, \beta = 1, b = \gamma \oplus \delta, c = \theta(\gamma \oplus \delta) \oplus \eta$, there is a deterministic output of $A = 1$. There are four extremal points in this case. We list the conditional probability distributions of $p(a, b, c|x)$ in Table III.

Case 3: When $\alpha = 1, \beta = 0$, there is a deterministic output of $A = X$. Consequently, $b = \gamma X \oplus \delta$. There are twelve extremal points in this case. We list the conditional probability distributions of $p(a, b, c|x)$ in Table IV.

Case 4: $\alpha = \beta = 1$. There are twelve extremal points in this case, which coincide with the ones in Case 3 up to a flip. We list the conditional probability distributions of $p(a, b, c|x)$ in Table V.

Afterwards, we can set up a linear programming optimization to test whether Eq. (20) can be written as a convex combination of these extremal points. It can be easily checked that this is not possible, hence proving that the probability distribution in Eq. (20) is outside $\mathcal{C}(G)$.

	000	001	010	011	100	101	110	111
X=0	1							
X=1	1							
X=0		1						
X=1		1						
X=0			1					
X=1			1					
X=0				1				
X=1				1				

TABLE II. Conditional probabilities of the extremal points in Case 1.

	000	001	010	011	100	101	110	111
X=0					1			
X=1					1			
X=0						1		
X=1						1		
X=0							1	
X=1							1	
X=0								1
X=1								1

TABLE III. Conditional probabilities of the extremal points in Case 2.

	000	001	010	011	100	101	110	111
X=0	1							
X=1					1			
X=0		1						
X=1						1		
X=0			1					
X=1							1	
X=0				1				
X=1								1
X=0	1							
X=1							1	
X=0		1						
X=1								1
X=0			1					
X=1					1			
X=0				1				
X=1						1		
X=0					1			
X=1						1		
X=0			1					
X=1						1		

TABLE IV. Conditional probabilities of the extremal points in Case 3.

	000	001	010	011	100	101	110	111
X=0					1			
X=1	1							
X=0							1	
X=1		1						
X=0								1
X=1			1					
X=0				1				
X=1								1
X=0							1	
X=1	1							
X=0								1
X=1		1						
X=0								1
X=1	1							
X=0							1	
X=1		1						
X=0						1		
X=1			1					
X=0				1				
X=1							1	
X=0								1
X=1								1

TABLE V. Conditional probabilities of the extremal points in Case 4.

-
- [1] J. Pearl, *Causality: Models, Reasoning, and Inference, 2nd ed.* (Cambridge University Press, Cambridge, England, 2009).
- [2] Č. Brukner, [Quantum \[un\] speakables II: half a century of Bell's theorem](#), 95 (2017).
- [3] A. Einstein, in *The meaning of relativity* (Springer, Dordrecht, 1922) pp. 54–75.
- [4] J. Pearl and T. Verma, in *Proceedings of the Sixth National Conference on Artificial Intelligence - Volume 1, AAAI'87* (AAAI Press, 1987) p. 374–379.
- [5] J. Pearl, *Biometrika* **82**, 669 (1995).
- [6] J. Tian and J. Pearl, in *Proceedings of the Eighteenth conference on Uncertainty in artificial intelligence* (2002) pp. 519–527.
- [7] R. J. Evans, *Ann. Stat.* **46**, 2623 (2018).
- [8] T. S. Richardson, R. J. Evans, J. M. Robins, and I. Shpitser, *Ann. Stat.* **51**, 334 (2023).
- [9] D. Geiger and J. Pearl, in *Uncertainty in Artificial Intelligence*, Machine Intelligence and Pattern Recognition, Vol. 9, edited by R. D. Shachter, T. S. Levitt, L. N. Kanal, and J. F. Lemmer (North-Holland, 1990) pp. 3–14.
- [10] T. Verma and J. Pearl, in *Uncertainty in Artificial Intelligence*, Machine Intelligence and Pattern Recognition, Vol. 9, edited by R. D. Shachter, T. S. Levitt, L. N. Kanal, and J. F. Lemmer (North-Holland, 1990) pp. 69–76.
- [11] D. Geiger, T. Verma, and J. Pearl, in *Uncertainty in Artificial Intelligence*, Machine Intelligence and Pattern Recognition, Vol. 10, edited by M. Henrion, R. D. Shachter, L. N. Kanal, and J. F. Lemmer (North-Holland, 1990) pp. 139–148.
- [12] J. Robins, *Math. Model.* **7**, 1393 (1986).
- [13] T. Verma and J. Pearl, in *Proceedings of the Sixth Annual Conference on Uncertainty in Artificial Intelligence* (1990) pp. 255–270.
- [14] J. J. Sakurai and J. Napolitano, *Modern quantum mechanics* (Cambridge University Press, 2020).
- [15] J. S. Bell, *Physics Physique Fizika* **1**, 195 (1964).
- [16] J. F. Clauser, M. A. Horne, A. Shimony, and R. A. Holt, *Phys. Rev. Lett.* **23**, 880 (1969).
- [17] J. Barrett, *Phys. Rev. A* **75**, 032304 (2007).
- [18] G. Chiribella, G. M. D'Ariano, and P. Perinotti, *Phys. Rev. A* **81**, 062348 (2010).
- [19] P. Janotta and H. Hinrichsen, *J. Phys. A: Math. Theor.* **47**, 323001 (2014).
- [20] S. Popescu and D. Rohrlich, *Found. Phys.* **24**, 379 (1994).
- [21] A. Acín and L. Masanes, *Nature* **540**, 213 (2016).
- [22] M. L. Almeida, J.-D. Bancal, N. Brunner, A. Acín, N. Gisin, and S. Pironio, *Phys. Rev. Lett.* **104**, 230404 (2010).
- [23] S. Lauritzen, “Graphical models oxford statistical science series 17, 1996.”
- [24] B. S. Cirel'son, *Lett. Math. Phys.* **4**, 93 (1980).
- [25] J. Henson, R. Lal, and M. F. Pusey, *New J. Phys.* **16**, 113043 (2014).
- [26] R. J. Evans, *Scand. J. Stat.* **43**, 625 (2016).
- [27] T. S. Richardson and J. M. Robins, Center for the Statistics and the Social Sciences, University of Washington Series. Working Paper **128**, 2013 (2013).
- [28] P. G. Wright, *The tariff on animal and vegetable oils*, 26 (Macmillan, 1928).
- [29] T. Van Himbeeck, J. Bohr Brask, S. Pironio, R. Ramanathan, A. B. Sainz, and E. Wolfe, *Quantum* **3**, 186 (2019).
- [30] J.-W. Pan, D. Bouwmeester, H. Weinfurter, and A. Zeilinger, *Phys. Rev. Lett.* **80**, 3891 (1998).
- [31] A. J. Short, S. Popescu, and N. Gisin, *Phys. Rev. A* **73**, 012101 (2006).
- [32] E. Wolfe, R. W. Spekkens, and T. Fritz, *J. Causal Inference* **7**, 20170020 (2019).
- [33] E. Wolfe, A. Pozas-Kerstjens, M. Grinberg, D. Rosset, A. Acín, and M. Navascués, *Phys. Rev. X* **11**, 021043 (2021).
- [34] N. Gisin, J.-D. Bancal, Y. Cai, P. Remy, A. Tavakoli, E. Zambrini Cruzeiro, S. Popescu, and N. Brunner, *Nat. Commun.* **11**, 2378 (2020).
- [35] R. Chaves, G. Carvacho, I. Agresti, V. Di Giulio, L. Aolita, S. Giacomini, and F. Sciarrino, *Nat. Phys.* **14**, 291 (2018).
- [36] M.-O. Renou, E. Bäumer, S. Boreiri, N. Brunner, N. Gisin, and S. Beigi, *Phys. Rev. Lett.* **123**, 140401 (2019).
- [37] P. Lauand, D. Poderini, R. Nery, G. Moreno, L. Pollyceno, R. Rabelo, and R. Chaves, *PRX Quantum* **4**, 020311 (2023).
- [38] D. Deutsch and C. Marletto, *Proc. R. Soc. A: Math. Phys. Eng. Sci.* **471**, 20140540 (2015).
- [39] C. Marletto and V. Vedral, *Phys. Rev. D* **102**, 086012 (2020).
- [40] G. Chiribella, G. M. D'Ariano, and P. Perinotti, *Phys. Rev. A* **84**, 012311 (2011).
- [41] H. Barnum, J. Barrett, L. O. Clark, M. Leifer, R. Spekkens, N. Stepanik, A. Wilce, and R. Wilke, *New J. Phys.* **12**, 033024 (2010).
- [42] P. Janotta and R. Lal, *Phys. Rev. A* **87**, 052131 (2013).
- [43] E. C. Stueckelberg, *Helv. Phys. Acta* **33**, 458 (1960).
- [44] E. B. Davies and J. T. Lewis, *Commun. Math. Phys.* **17**, 239 (1970).
- [45] M. Ozawa, *J. Math. Phys.* **25**, 79 (1984).
- [46] J.-M. A. Allen, J. Barrett, D. C. Horsman, C. M. Lee, and R. W. Spekkens, *Phys. Rev. X* **7**, 031021 (2017).
- [47] J. Barrett, R. Lorenz, and O. Oreshkov, arXiv:1906.10726 (2019).
- [48] J. Barrett, N. Linden, S. Massar, S. Pironio, S. Popescu, and D. Roberts, *Phys. Rev. A* **71**, 022101 (2005).
- [49] P. Bierhorst, *J. Phys. A: Math. Theor.* **49**, 215301 (2016).